Optimization of the membrane distillation operation for desalination of the highly saline effluent generated during bioplastic production

*A Thesis submitted for the partial fulfillment of the continuous assessment of **Master of Technology** in **Environmental Biotechnology** course of **JADAVPUR UNIVERSITY** for the Session 2017-2019*

By

SAMPA BHOWMIK

Examination Roll No: M4EBT19007
Registration No: 141025 of 2017-2018
Roll No: 001730904001

Under the Guidance of

DR. JOYDEEP MUKHERJEE

UGC-Associate Professor
School of Environmental Studies
Jadavpur University

PROF. RAJA GHOSH

Professor
Department of Chemical Engineering
McMaster University
Hamilton, Canada

SCHOOL OF ENVIRONMENTAL STUDIES
JADAVPUR UNIVERSITY
KOLKATA: 700032

RECOMMENDATION CERTIFICATE

It is hereby certified that this **Thesis** titled **"Optimization of the membrane distillation operation for desalination of the highly saline effluent generated during bioplastic production"** is prepared and submitted for the partial fulfilment of the continuous assessment of **Master of Technology inEnvironmental Biotechnology** course of Jadavpur University by **Sampa Bhowmik** (Examination Roll No: M4EBT19007; Registration No: 141025 of 2017-2018; Roll No: 001730904001), a student of the said course for the session 2017-2019 under the joint supervision of **Dr. Joydeep Mukherjee**, UGC-Associate Professor, School of Environmental Studies, Jadavpur University and **Prof. Raja Ghosh**, Department of Chemical Engineering McMaster University, Hamilton, Canada**.**

_____

Dr. Pankaj Kumar Roy
Dean
Faculty of Interdisciplinary, Studies
Law & Management
Jadavpur University

_____

Dr. Pankaj Kumar Roy
Director
School of Environmental Studies
Law & Management
Jadavpur University

_____

Dr. Joydeep Mukherjee
(Thesis Supervisor)
UGC-Associate Professor
School of Environmental Studies
Jadavpur University

McMaster University

Department of Chemical Engineering

JHE-374
1280 Main Street West
Hamilton, ON L8S 4L7

Tel: 905.525.9140 Ext. 24292 / 24957
Email: chemeng@mcmaster.ca
http://www.chemeng.mcmaster.ca

May 23, 2019

Dear Sir or Madam:

This is to certify that SAMPA BHOWMIK, a student of the M. Tech. (Environmental Biotechnology) programme, run by the School of Environmental Studies at Jadavpur University, Kolkata, India was co-supervised by me, during the 2017-18 session. Her principal supervisor at Jadavpur University was Dr. Joydeep Mukherjee. Ms. Bhowmik's M. Tech. project was on "high-salinity water treatment using membrane distillation". Part of this work has been communicated as a research paper. During my interactions with Ms. Bhowmik I was very impressed with her diligence and dedication towards her work. I wish her the very best for her career.

Best regards

Raja Ghosh

Professor of Chemical Engineering

JADAVPUR UNIVERSITY
SCHOOL OF ENVIRONMENTAL STUDIES
KOLKATA: 700032

CERTIFICATE OF APPROVAL*

This is to certify that this thesis is hereby approved as an original work conducted and presented in a manner satisfactory to warrant its acceptance as a prerequisite to the degree for which it has been submitted. It is implied that by this approval the undersigned do not necessarily endorse or approve any statement made, opinion expressed or conclusion drawn therein, but approve the thesis only for the purpose for which it is submitted.

Final Examination for evaluation of thesis

1)……..

2)……..

3)……..

(Signature of Examiners)
* Only in case the thesis is approved

DECLARATION

This **Thesis** titled **"Optimization of the membrane distillation operation for desalination of the highly saline effluent generated during bioplastic production"** is prepared and submitted for the partial fulfilment of the continuous assessment of **Master of Technology in Environmental Biotechnology** course of Jadavpur University for the session 2017-2019.

_____

SAMPA BHOWMIK
Date:
Place: School of Environmental Studies
Jadavpur University
Kolkata: 700032

ACKNOWLEDGEMENT

I take this opportunity to express my sincere thanks and deepest sense of gratitude to **Dr. Joydeep Mukherjee**, UGC-Associate Professor, School of Environmental Studies, Jadavpur University who have supervised this thesis. The thesis would have never been completed without his able guidance, constant vigil, careful supervision and inspiration at all stages of the work.

I would like to express my gratitude to **Prof. Raja Ghosh**, Professor of Chemical Engineering, McMaster University, Hamilton, Canada, for his extensive guidance throughout the period of preparation of the thesis.

I would also like to express my gratitude to Dr. Pankaj Kumar Roy, Director, School of Environmental Studies and other respected teachers of the School of Environmental Studies for the continuous encouragement, support and valuable advice they provided throughout my work.

I would like to personally express my appreciation to Sayak Bhattacharya, Dhruba Bhattacharya and Sayantani Basu, the research scholars of the School of Environment Studies, Jadavpur University for providing helps as and when necessary.

I would also like to thank Mr. Debasis Das, all the librarians, assistant librarians and library staffs of the Central Library and the Departmental Library of Jadavpur University for their kind cooperation during preparation of this thesis by providing me the books and documents as and when necessary.

Last, but not the least, I express my gratitude to Biswajit Chakraborty, Moumita Saha, Bishal Ghosh, Swarnendu Shekhar Das, my friends and my family for the encouragement and support they provided throughout the work. This thesis would not have been possible without them.

Sampa Bhowmik
Roll No. 001730904001
Examination Roll No.: M4EBT19007
Date:
Place: School of Environmental Studies
Jadavpur University
Kolkata: 700032

Abstract

The objective of this project was to investigate the process parameters of direct contact membrane distillation (DCMD) for desalination of the highly saline spent media generated by halophilic *Haloferax mediterranei*, a producer of polyhydroxyalkanoate bioplastic. The experimental runs were conducted with polytetrafluoroethylene (PTFE), polypropylene (PP) polyvinylidene fluoride (PVDF) membranes each having pore sizes 0.22 µ, 0.45 µ and 1.0 µ. The feed solution was mainly aqueous saline solution with high TDS value of 225.5 gm/lit. This study observed that higher feed temperature exhibited better mass flux through the membrane, whereas conductive heat loss reduced the temperature gradient which subsequently reduced the flux. Reheating the cooled brine reject from the hot exit maintained the steady ΔT value throughout the process thus lowering the time for crystallization of salts. PTFE showed high maximum (21.3 lit/m^2hr.) and average flux (16.9 lit/m^2hr.) when the ΔT value was 85 ºC. However, in case of PVDF it showed similar mass flux (maximum 25.1 lit/m^2hr.; average 18.3 lit/m^2hr.), despite lowering the ΔT by 20 ºC. The crystallization time for both PTFE and PVDF were more or less same, 3.0 hr. and 3.25 hr. respectively. Low operating ΔT, high contact angle, high surface energy and low conductivity of PVDF showed better process efficiency than PTFE and PP. Moreover, it has been observed that increase in TDS reduced the mass flux, as the non-volatile salt deposited in the pores and hence reduced the permeability of the membrane. Pore diameter did not influence the flux rate.

CONTENTS

Chapter 1
Introduction

Chapter 1

1. Introduction

1.1. Environment

Environment is a natural complex system comprising with all living and non-living components which are present naturally on the earth. Environment is the interaction between physical, chemical and biotic factors of surroundings that affects an organism or population in their survival including growth and evolution.

In contrast to this natural environment people have constructed artificial environment that are influenced human life strongly. Along with this built environment; the climate, temperature, weather, resources, light etc. all influence any species with in its environment. So, all living entities have to adopt its condition of the environment. In last century, scientists have been discovered that people are causing pollution of natural resources, deforestation, acid rain, plastic pollution and other problems by their anthropogenic activities that are dangerous for both human life and natural environment.

1.2. Environmental pollution

Environmental pollution can be defined as the alteration of any constituent or introduction of any contaminants which causes adverse condition to the natural environment. The components of pollution can be either chemical, physical, biological natural sources or anthropogenic activities. Depending on the nature of source, pollution is often classified as point source and nonpoint source.

A point source is a type of pollution where one particular source of air, water, or land is polluted. This pollution is less harmful than nonpoint source, as it can be distinguished from other pollution sources significantly. Moreover, point source can be analyzed particularly by mathematical modelling.

Nonpoint source (NPS) pollution refers to the mixing of two or several resources in a diffuse manner. Nonpoint source pollution affects a water body from sources such as polluted runoff from agricultural areas draining into a river; also it causes land pollution due to the irregular usage of chemical fertilizers.

Pollutions of biotic and abiotic components (land, water, air etc.) may lead to potential changes in the global geochemical cycles of abiotic components as well as the sustainable habitation of humans and other organisms. Even though other organisms are the worst sufferers from the adverse effects of natural changes, however, the main culprit is the uncontrolled human activities. The hazardous substances are generated from various industries, chemical fertilizers, hospitals, etc. and gradually entering in the natural environment system which leads to alteration of the entire living systems along with many critical changes in the environment (Kampa et al. 2008). Urbanization has been a constant

global problem from last century. Huge constructions of industries, which are using non-renewable resources, are experiencing problems with waste management, crisis of fossil fuels, increasing pollution etc. (William et al. 2011). DDT is one of the major toxic chemical which affects the living organism badly. Likewise, car exhaust gases alter the composition of biosphere and increases harmful gases that damage health of both adults and children, leading to change in behavior and psycho-social development of children (Markert et al. 2011).

1.3. Plastic

The unprecedented growth in population and development in conventional plastic industry has produced an immense amount of waste plastic solids for which the society was unprepared. Plastics are a wide range of synthetic or semi synthetic polymeric substances derived from fossil based carbon sources. It has become a part and parcel of our day to day life due to its easy availability, versatility and imperviousness to water. The widespread usage of conventional plastic causes fossil fuel crisis, also increases the solid plastic waste which may take several years to degrade.

Plastics play a key role in almost every aspect of our daily lives. Plastics are hugely used for manufacture of daily used products such as beverage containers, toys, and furniture. The widespread and irregular usage of plastics demands proper "end-of-life" management. The largest amount of waste plastics are generated as containers and packaging materials (e.g. soft drink bottles, lids, shampoo bottles), but these also are found in durable (e.g. appliances, furniture) and nondurable goods (e.g. diapers, trash bags, cups and utensils, medical devices) that requires several months to degrade.

The widespread utilization of synthetic plastic within our society is due to its durability, thermal and mechanical properties as well as these synthetic plastic are very cheap. The extensive global usage of plastics has contributed heavily to environmental pollution; as the solid waste plastics are not always recycled properly and consequently enters within the environment geochemical systems. The manufacturing processes also produce large quantities of hazardous pollutants. In recent years people has been conscious about the negative effect of this plastic pollution, people becoming more aware of these environmental issues. Thus, it is the high time to develop new technologies to produce non-petroleum based sustainable resource material. Bioplastics are one of the potential substitutes, as they are carbon neutral and biodegradable in nature. Presently, bioplastics are not economical as compare to fossil-based conventional plastics.

Fig.1. Plastic pollution

1.4. Plastic pollution

The major plastic pollution occurs due plastic bags only; it contributes mostly as these bags are extremely durable and cheap. These plastic bags have led this pollution to a critical level. The main demerit of these plastic bags is that they are non-renewable in nature. These plastic materials are derived from carbon based non-renewable sources which impending the fossil fuel crisis gradually. Plastic bags are not easily recycled as paper bags. It can last for as much as hundreds of years in the environment.

1.5. Threat to animal life

As per Marrickville Council of Australia, it was reported that 100,000 whales, turtles and birds die have been died every year, mainly because of consumption of plastic materials. Plastic bags not only have adverse effects on our natural habitats, but have also been found to be responsible for the death of many animals, mainly on account of the suffocation encountered on eating them. Not only animals, infants and young children have also been reported to have lost their life, on account of plastic bags. Since plastic bags are thin and airtight as well, children often end up blocking their mouths and nostrils with them. In case they are not being monitored by an adult, this leads to suffocation and, in some cases, even death.

Fig.2. Effect of plastic pollution in the ocean

1.6. Bioplastic

The bioplastic or bio based plastics are eco-friendly as they are biodegradable, biocompatible and most important is they are self-sustainable. They reduce the consumption of conventional fossil fuel resources. Bio plastics can be easily derived from renewable biomass sources, such as ethanol based waste effluent, vegetable fats and oils, molasses, corn starch. Microorganisms and algae are the common strains mostly degraded organic waste to form bio plastic.

Fig.3. Biodegradable utensils, bottles, packaging materials made from bioplastics

Bio based plastics are carbon neutral they don't emit carbon dioxide. Despite of such advantages the bioplastics are not strongly popular in the plastic world. This is because, these bioplastics has less superior qualities than synthetic plastics. Hence, it becomes a prime focus to the scientists and engineers to make its properties more powerful and improvised "Green composition"(Pilla et al. 2010) is a blending process where bioplastics are blended with natural fiber to produce 100% biodegradable substitute. However, researchers also trying to

blend bioplastic with synthetic polymers to meet outstanding properties, also it will reduce the carbon footprint.

A number of different biodegradable bio-based polymers can be derived by different microbial activity; some of these are Polyhydroxyalkanoates (PHAs), aliphatic polyesters, polyhydroxybutyrate, bio-derived polyethylene, polylactides (Lee et al. 1996). These bioplastic reduces the solid waste management problems. Among these, PHAs, is the most common polymer as it can be produced by a wide variety of microbial strains and its property is similarity to conventional plastics and degraded completely over a short period of time (Anderson et al. 1990). Hence, its production methods, extraction process, effluent treatment, overall cost reducing techniques have become a main stream study area nowadays.

Fig.4. An illustration of the time taken for biodegradable plastic to degrade

1.7. Present status of bioplastic and its future aspect

Since the large scale production cost of bioplastic is very much costly so it has not been commercialized extensively. During 20th century the bioplastics was mainly produced by the developed countries like North America, Japan, and Western Europe etc. The concept was very new to the world, though its production process was easy but it required high processing cost for its purification. On the basis of this study, it has been reported that, Brazil has been one of the largest producer of bioplastic in the year of 2013. In Japan, the demand of bioplastics was very high so they produced more than 178000 metric tons in 2013. China has planned to produce 100,000 metric tons of bioplastics by 2013. A research work carried out by BCC has revealed a fact that the bioplastics market value has reached 541 million pounds in 2007, which increased to 1.2 billion pounds in the year of 2012. In 2008, the demand of biodegradable plastics like polylactic acid, resins, polyesters etc. has been accounted for about 90% of total bioplastics production. Biodegradable plastics are less harmful to the environment and can degrade very fast. It reduces in emission of CO_2 compared to conventional synthetic plastics. The production cost of bioplastics is also too high compare to

the traditional plastic. This is one of the major problems related to bioplastics development. The cost of per Kg bioplastic is around 1.3 to 4 Euros.

Haloferax mediterranei is one of the index organisms which are nowadays employed for the mass production of bioplastic (polyhydroxyalkanoates). These haloarchaea requires hypersaline media for their growth and activity. However, the problem is that, this hyper saline spent media needs to be desalinated after the extraction of bioplastic cells. Previously, decanoic acid was employed for two step desalination of the spent stillage medium in a cylindrical baffled-tank with an immersed heater and a stirrer holding axial and radial impellers (Bhattacharyya et al. 2014). Though the purpose of desalination was fulfilled but it enhances the overall production cost. So, Direct Contact Membrane Distillation (DCMD) is introduced to treat the spent stillage generated during the bioplastic production to make the process economical.

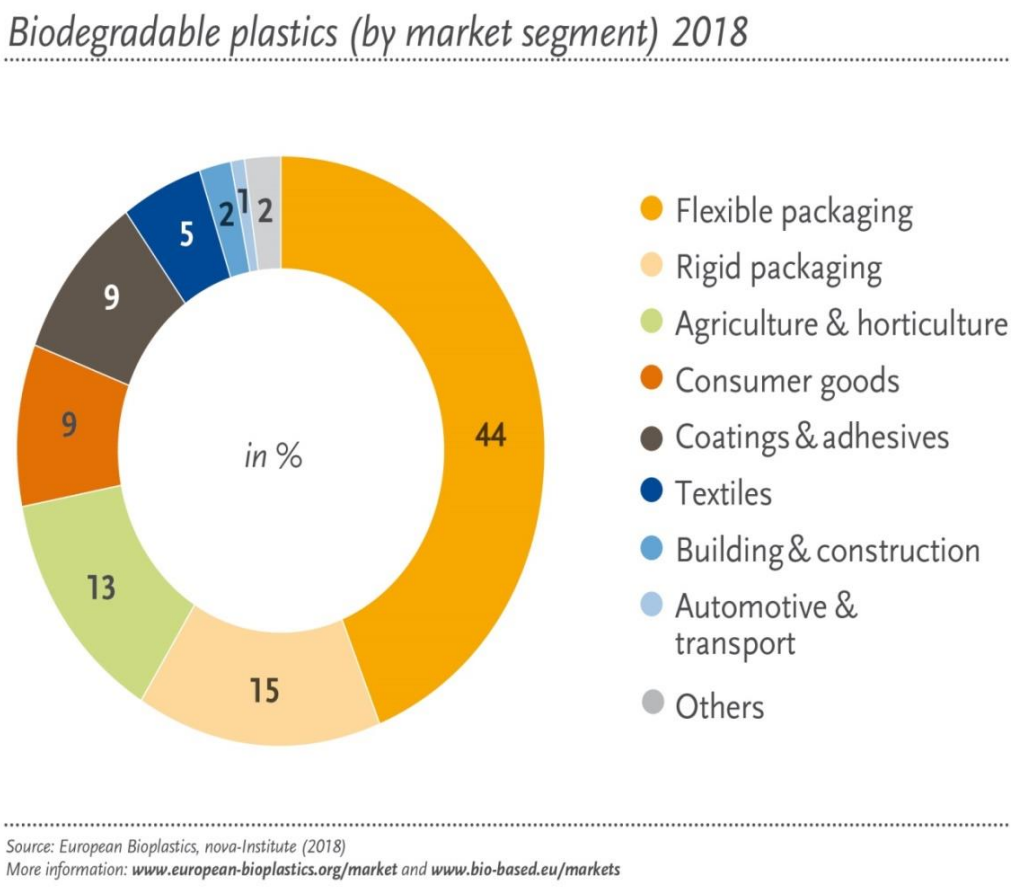

Fig.5. Graphical representation of bioplastic usage in 2018

1.8. Membrane technology

Membrane technology is currently of prime focus in several treatment processes of water and polluted effluents of many developed countries because of the numerous advantages of membrane separation based on thermal technologies (Jevons et al. 2010). Some of these benefits are the savings of thermal energy (Lee et al. 2011), reduction of negative impacts on environment associated with reduction of carbon footprint of fuel combustion for thermal energy production, lowering of capital requirements. However, reverse osmosis (RO) is an established membrane separation process have also been shown to be susceptible to challenges such as a near inverse relationship between membrane selectivity and permeability (Giwa et al. 2016) , higher requirement of energy and membrane fouling occurs during desalination of highly saline feed(Elimelech et al. 2011). In such cases, higher levels of feed pretreatment require. Many membranes are enabling to remove different micro pollutants and contaminants of feed water because those can only separate only particular type of pollutants. Therefore, membrane separation has been integrated with thermal distillation in order to combine the benefits of both approaches; this new concept is known as membrane distillation (MD) (Drioli et al. 2015).

Membrane Distillation (MD) is a thermally based separation process of removing micro pollutants, salts, heavy metals etc. from an aqueous solution, making it distilled through a semi permeable hydrophobic membrane. Nowadays, MD technology has become a first-line choice for different water treatment processes as well as for different industries. In this thermally driven process, a hydrophobic membrane separates a hot feed stream and a relatively cold permeate stream which results a temperature difference in two sides of the membrane. This temperature gradient across the porous membrane creates a vapor pressure difference; this is the main driving force for mass and heat transfer across the membrane. The porous membrane allows only the volatile molecules and the non-volatile molecules are concentrated in the hot feed side. One of the major advantages of this process is that, it can be operated at very low temperature range which is below the boiling point of the feed solution.

Membrane distillation process was introduced in the year of 1960s (Susanto et al. 2011). But that time it was not commercialized due to (1) high price of the membrane material (2) the installation cost is also high so; the whole process was not economical at that time. After that a lot of research and investigations have been done to make this process efficient and commercially available. MD has several advantages:

(1) Energy requirement is very less. Renewable energy like solar energy, geothermal energy, and low chemical energy can be engaged instead of conventional energy.
(2) The osmotic pressure of highly saline feed solution does not affect the process.
(3) It can be operated at a very low hydrostatic pressure.
(4) It works at very high concentration near to saturation point.
(5) Salt rejection capacity is high and less responsive to feed concentration.

In spite of these advantages, MD is not fully scaled-up yet, it needs to be applied widely in different industries. The membrane should have high liquid entry pressure, low thermal conductivity and high permeability for movement of the vapor molecule from feed side to permeate phase.

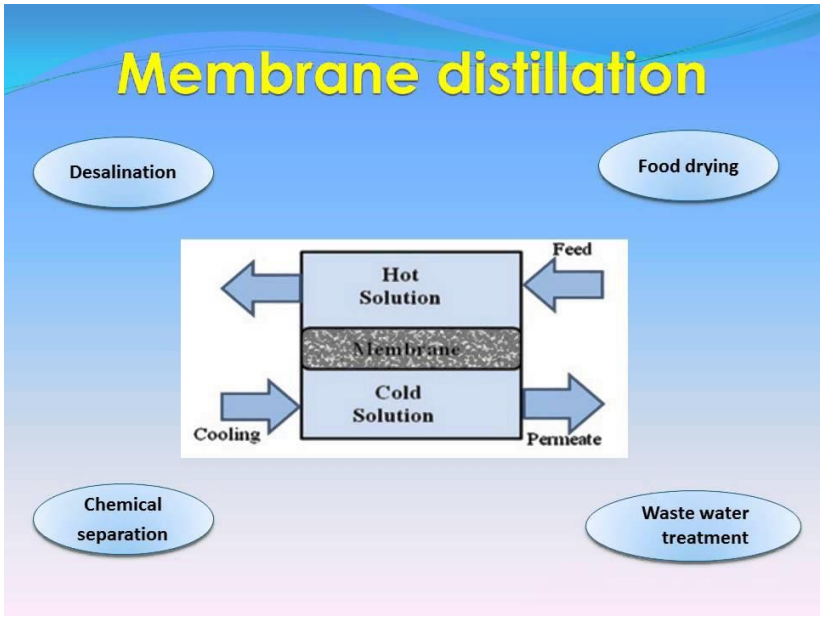

Fig.6. Membrane technology

1.9. Current issues of Membrane Technology

Current issues of MD for separation processes involving the lower productivity of MD membranes due to the pore wetting difficulty (Susanto et al. 2011). To avoid pore wetting, the transmembrane hydrostatic pressure should be lower than the liquid entry pressure (LEP). The lower pressure causes the transfer of water molecule through the porous membrane instead of vapor molecules. Higher external pressure beyond the acceptable limit would cause severe problems like pore wetting, membrane fouling, and low solute rejection (Tijing et al. 2015, Warsinger et al. 2015). Lack of proper fabrication of the membranes for commercial MD applications is sometimes responsible for current issues affecting MD membrane performance, as membranes designed for conventional membrane technologies (such as microfiltration or MF and ultrafiltration or UF) are currently being used for most MD investigations. In addition, energy inefficiency is another concern in many MD applications currently because energy is lost due to temperature polarization and heat of condensation at the cold (permeate) side. Heat is also transferred readily as soon as the hot and cold fluids are comes in contact of both side of the membrane interface. Although the partial vapor pressure for mass transfer can be improved by using renewable energy, especially solar thermal energy.

1.10. Problem investigated

Haloferax mediterranei is one of the common halophilic microbial strains widely used in industrial scale for production of PHA. It is highly economical because it can utilize cheap carbon sources, also has the capacity for nonsterile cultivation and the product recovery is relative simple. These large scale industries mainly used sources like molasses, vegetable oils, hydrolyzed water, cereal stillage which are rich in nutrient. Activated sludge process is followed for mass cultivation of the organism. In this process, the organism slowly consumes the carbon source and accumulated 63 ± 3 % PHA in their cell and synthesized 13.12 ± 0.05 g of PHA/l (Bhattachariya et.al). The product yield coefficient was 0.27 while 0.14 g/l h.

The high salt concentration in this PHA production medium of extreme halophiles allows a process without sterilization, but its disposal after the end of a batch or fed-batch cultivation is a massive problem as the present environmental standards do not allow this high TDS discharge irregularly without post treatment processes. Bhattacharyya et al.(2014) applied water soluble decanoic acid for two-stage desalination of the spent stillage medium generated after production of the PHA poly-3-(hydroxybutyrate-co-15.4 mol%-hydroxyvalerate) (PHBV) by *Haloferax mediterranei*. This process was first performed in a beaker and subsequently the whole process was scaled up in a cylindrical baffled-tank with an immersed heater and a stirrer holding axial and radial impellers (Bhattacharyya et al. 2015). Although, this process rejected 99.3 % of the medium salts which were re-used for PHA production, but this process may not be suitable further higher scales due to the higher cost of decanoic acid and the operational difficulties of the recycling the directional solvent. Hence, in this present study we introduced DCMD as an alternative methodology for removal and concentration of medium salts after PHA production by *Haloferax mediterranei*.

1.11. Objectives

The current project aimed to investigate the application of Direct Contact Membrane Distillation for desalination of the growth media of *Haloferax mediterranei* and to optimize membrane efficiency with varying temperature gradients. The main focus of the work includes:

- Optimization of temperature gradient by varying the feed temperature (70 -90ºC) and permeate temperature (5-25ºC).
- Comparative study of permeate flux for PP, PTFE, PVDF membranes.
- Optimization of effects of temperature on feed solution for flux generation.
- Determination of crystallization time.

Chapter 2
Review of literature

Chapter 2

2. Review of literature

2.1. Chemical structure of PHA

Generally the basic structure of PHAs consists of 3-hydroxy fatty acids as shown in Fig.7.Each monomer contains a side alkyl group. The pendant R group varies in their nature; mostly it is saturated but can be also present as unsaturated, branched or substituted form. Based on the functional *R* group, the nomenclature and carbon numbering is done. The most common polymers and their varying R groups are shown in Table 1.

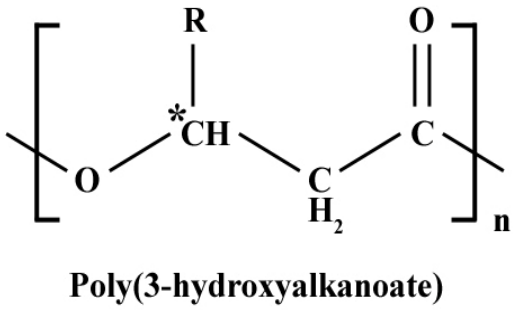

Fig.7. Chemical structure of polyhydroxyalkanoate

Table 1: Types of PHA

R Group	Full name	Carbon no
CH_3	Poly(3-hydroxybutyrate)	C_4
CH_2CH_3	Poly(3-hydroxyvalerate)	C_5
$CH_2CH_2CH_3$	Poly(3-hydroxyhexanoate)	C_6
$CH_2CH_2CH_2CH_3$	Poly(3-hydroxyheptanoate)	C_7

Different microorganisms synthesized varieties of molecular mass of PHA during different stage of production process and condition. The largest reported molecular mass of PHA is about 20 MDa reported by (Kusaka et al. 1997). As these biochemical reactions are pH sensitive, it can directly affect the nature and size of the molecular mass produced by the culture. Also, the type and concentration of the carbon source has a great effect on the morphology of molecular mass of PHA.

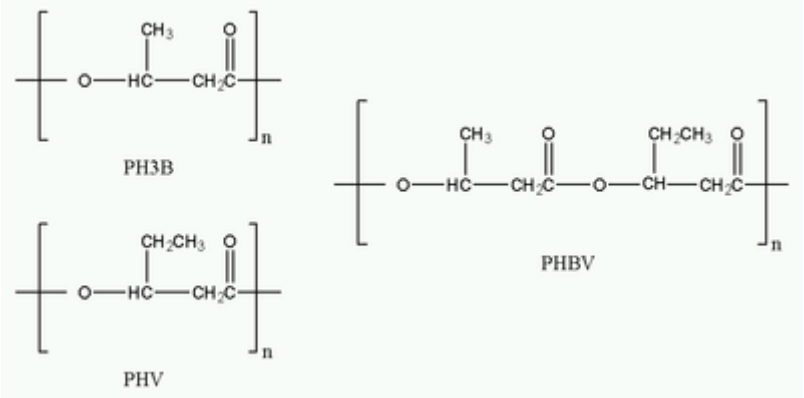

Fig.8. Chemical structure of some polyhydroxyalkanoates, a) PH3B, b) PHV, c) PHB

2.2. Properties of biopolymers

These biocompatible polymers are thermoplastic in nature and vary widely in their different characteristics according to the chemical composition and structure it poses. PHB shows effective resistivity against moisture and aroma barrier properties. If PHB materials are stored for long time in room temperature it's become fragile and brittle due to its re-crystalline property. It has been also reported that the samples stored in room temperature for 60 days shows poor mechanical property than the samples stored in same condition for 30 days. This proves that bioplastics can be easily degraded naturally. The stress/strain graph of PHB samples stored at 50% RH for respectively 30 and 60 days, and stored at low temperature (HR) (5°C) are shown below (Bugnicourt et al. 2014).

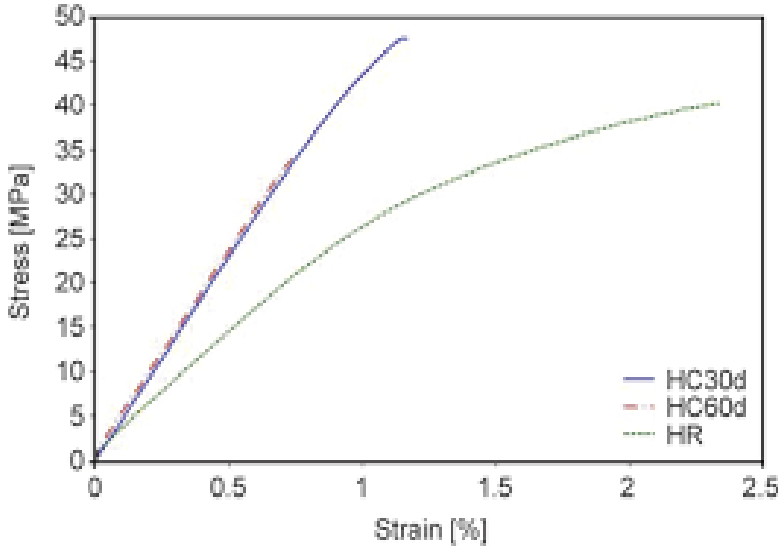

Fig.9. Stress /strain of PHB (H) samples stored at 50% RH for respectively 30 (HC30d) and 60 days (HC60d), and stored at low temperature (HR)

2.3. PHA Storage in Cell

PHAs bio accumulated as intercellular lipid granules in the microbial cell. These PHA molecules acts as energy reserves in nutritional depletion condition .It promote the long term survival in such nutrient stress condition. The different characteristics of the PHA granule e.g. type of PHA, the number and size of granules and the morphology are dependent upon the microorganism's characteristics (Davey et al. 2002) As PHAs, are lipid in nature, it insoluble in water and therefore the polymers are easily accumulated as intracellular granules. PHA is produced in presence of excess carbon which maintains the osmotic balance in the cell. These intercellular granules don't interact with the cell constituent. PHAs can be accumulated as high as 90% (w/w) of the dry cell mass of the bacterial cell (Fig. 10).

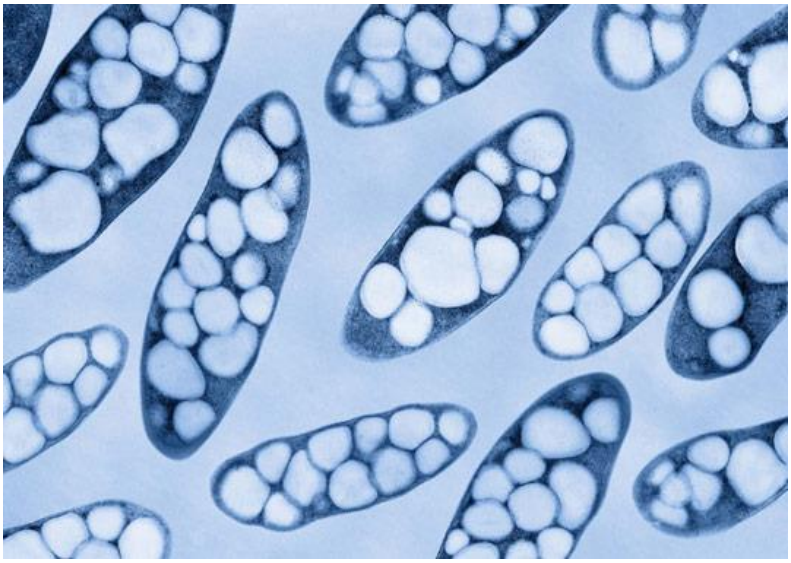

Fig .10. PHA storage in cell

2.3.1. Archaea

The archaea species which contribute greatly in production of PHA are mostly haloarchaeal species of different genera *Haloferax*, *Halalkalicoccus*, *Haloarcula*, *Halobacterium*, *Halobiforma*, *Halococcus*, *Halopiger*, *Haloquadratum*, *Halorhabdus*, *Halorubrum*, *Halostagnicola*, *Haloterrigena*, *Natrialba*, *Natrinema*, *Natronobacterium*, *Natronococcus*, *Natronomonas*, and *Natronorubrum.* These can tolerate extreme halophilic condition. These require high salt activity for their normal enzyme activity, upto 6 M NaCl. The substrates which are suitable for haloarchaea are glucose, volatile fatty acids, whey hydrolysate, vinasse, crude glycerol etc. The PHA which produced is exclusively short chain length in nature.

Presently, *Haloferax mediterranei* is one of the best producers of PHA as it does not require high optimum growth condition. Due to Halophilic in nature it requires 2 to 5 M NaCl for their growth and enzyme activity. Its produces a high amount of PHA levels between 50 and 76 %CDM. *H. mediterranei* is one of the attractive candidates for synthesis of PHA as

they can tolerate hypersaline conditions, required for its growth and enzyme activity. This will produce highly purified PHA products as other organisms can't survive in such extreme halophilic condition. Hence, it will reduce the production cost. (i.e., process piping, instrumentation and insulation, electricity for steam generation, etc.) (Bhattacharyya et al. 2012). However, in extreme salinity corrosion of stainless steel may take place (Quillaguaman et al. 2005). Haloarchaea are more economical than halophilic bacteria for its easy recovery of PHA. Different methods are applied for recovery of PHA from halophilic bacteria – chemical, physical (mechanical) enzymatic. Firstly, cell wall is disrupted to release intracellular PHA granules; this is one of the vital steps which could account more than 50% of the overall production cost (Chen et al.2001). Extraction is followed by cell lysis. This solvent extraction requires organic solvents like chloroform and acetone which are considered as potential environmental hazardous compound if their detoxification and disposal are not mismanaged. Conversely, the recovery of PHA for haloarchaea is relatively easy -cell lysis in distilled water, released PHA granules is then recovered by centrifugation (Poli et al. 2011). This makes PHA recovery relatively cost effective, less chemical- and energy requirement, lower extraction cost, lower ecological footprint.

2.4. Membrane Distillation (MD) configuration

MD has four basic configurations depending on the difference in the receiving phase; DCMD (Direct contact membrane distillation), AGMD (Air gap membrane distillation), SGMD (swap gas membrane distillation), and VMD (vacuum membrane distillation). Among these four configurations, DCMD has gained more popularity in bench scale laboratory based research works. It does not require an external condenser and it is more suitable for water based applications (Pangarkar et al.2011). DCMD has been studied widely due to its simplest configuration and the operational process of DCMD is relatively easy and high flux can be obtained at the right operating conditions.

In DCMD, the feed solution and the permeate liquid are in direct contact with the membrane. DCMD requires very low thermal efficiency as the evaporation and the condensation surfaces are very close to each other. The polymeric membrane separates hot feed and the cold permeate, the temperature difference in both sides of the membrane generates temperature polarization coefficient which is the main driving force here. This temperature polarization leads to simultaneous movement of volatile molecules and heat from concentrated feed side to the permeate side.

AGMD requires higher thermal energy utilization but generates lower flux. SGMD also exhibits high thermal efficiency but huge amount of sweeping gas is required to produce high permeate recovery. VMD can be used for both considerable thermal efficiency and permeate flux but the set-up procedure for VMD is quite complicated, mainly because of the vacuum and external condensers parts (Koo et al. 2013).This is the main drawback of VMD. Like DCMD, the productivity and the flux of VMD can also be improved by increasing the feed temperature and other operational parameters (Alkhudhiri et al. 2012).

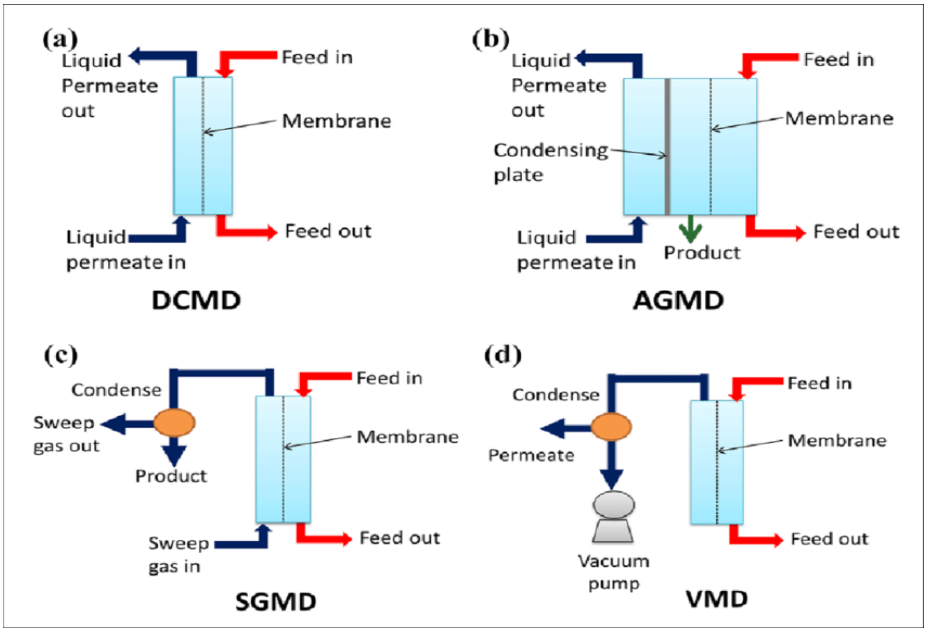

Fig.11.Configuration of DCMD

Table 2: Advantages and disadvantages of MD configuration

MD configuration	Pros.	Cons.
• DCMD	• Easy and simple	• High conductive heat loss
• AGMD	• Low conductive heat loses	• Low permeate flux • Additional resistance to mass transfer is created
• SGMD	• Low conductive heat loses	• Difficult module design
• VMD	• High permeate flux	• Difficult heat recovery • Higher possibility of pore wetting

2.5. Characteristics of membrane distillation

The membrane distillation process should have the following characteristics (Smolders et al. 1989):

- The membrane should be porous in nature.
- The membrane should be hydrophobic so that it should not be penetrated with the process liquids.
- Pores of the membrane should not be blocked by capillary condensation.

- The porous membrane should only allow the vapor molecules to be transported through it.
- The vapor/liquid equilibrium of the different components in the process liquids must be maintained by the membrane
- For each component the driving force of this membrane operation is the partial vapor pressure gradient

2.6. Working principle of Direct contact membrane distillation (DCMD)

The MD arrangement utilized in this investigation is DCMD; therefore the main focus of this project lies on the working principle of this particular unit. The phenomena which take place in this DCMD process set-up involves (a) evaporation of hot solution at the feed side; (b) transportation of water vapor through the membrane pores due to trans-membrane vapor pressure difference, that is the driving force for this experimental process; (c) collection of the permeating water vapor by an inert cold water flow; and (d) condensation outside of the membrane module. In general, these phase change of water molecule carried out heat and mass transfer through the porous hydrophobic membranes simultaneously. The membrane only allows the mass transfer through its pores, while heat is transferred by both the membrane matrix and its pores. Conductive heat transfer takes place through the membrane material and heat transfer through the pores is due to latent heat of vaporization accompanying the vapor flux. In addition, fluid boundary layers are adjoining both the feed and permeate side which gives rise to the phenomena called temperature polarization and concentration polarization. In Fig.12 the temperature and concentration profile inside the DCMD is represented. The feed and cold permeate flow are in counter-current mode and tangentially to the membrane surface.

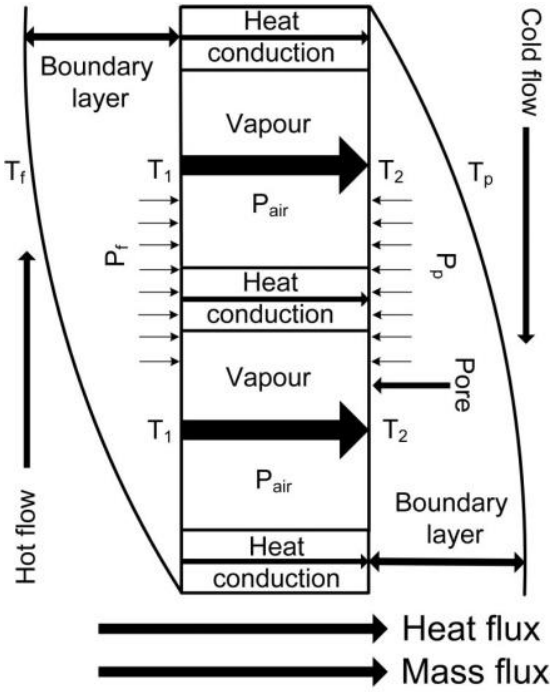

Fig.12. Heat transfer and mass transfer in DCMD through membrane (Camacho et al. 2013)

2.7. Theoretical Background

In the year of 1960s MD has been first introduced by Bodel. The driving force is different than other conventional processes such as RO. The vapor pressure difference in both hot and cold side is the main driving force for the heat and mass transfer through the membrane.

2.7.1. Temperature polarization

In MD process, heat and mass transfer occurs simultaneously from hot feed side to permeate side through the polymeric membrane. The heat is transferred mainly in two ways,

(1)The latent heat of evaporation for the transfer of vapor molecules from feed side to the cold side.

(2)Conductive heat transfer from hot side to cold as the hot feed and the chilled permeate fluid are in directly contact with the thin membrane surface layer.

The feed temperature T_f (Fig.12) drops across the boundary surface layer to T_1 of the membrane, as hot and cold fluids are in intimate contact of each other. A portion of feed water evaporates and transported through the membrane jointly with the latent heat of evaporation. Simultaneously, cold side temperature T_P, increases across the interface or boundary layer of the membrane surface to T_2 as hot feed water vapor condense to the permeate side and increases the temperature of the boundary layer permeate fluid flow. This vapor pressure difference between the boundary layer fluids, T_1 (hot side) and T_2 (cold side) is the main driving force for the mass transfer and heat transfer process (Camacho et al.2013).

The ratio of energy required for mass transfer of vapors (T_1- T_2) to total energy (T_f - T_P) is defined as temperature polarization coefficient. This coefficient τ is calculated as,

$$\tau = \frac{T1 - T2}{Tf - TP} \qquad (1)$$

The rate of condensation and evaporation depends on the temperature difference of the boundary layer /interface of the membrane, as the driving force that is the vapor pressure difference is a function of temperature difference. The difference between T_1 and T_2 affects the mass flux rate directly; the difference should be as high as possible for better mass flux generation. The temperature polarization coefficient can be enhanced by improving different operating parameters of membrane set up. Turbulence flow increases the TPC (Temperature polarization coefficient) by reducing thermal boundary layer. Spacer is used to improve flow characteristics between the DCMD module.

2.7.2. Heat transfer

Heat transfer in DCMD occurs in two routes. First one is sensible heat transfer from hot side to cold as a form of latent heat of evaporation. Due to the temperature difference between bulk fluid and the boundary layer vapor pressure difference generates, as a result some part of the volatile feed solution evaporates and takes latent heat of evaporation to pass across the membrane and condense in the permeate phase. Second one is conductive heat transfer due to the temperature difference generates by first step. The hot feed and the cold permeates are very close contact only separates by thin layer of polymeric membrane. So, this close contact formation causes conductive heat transmission.
Because the heat flux through the membrane is due to two mechanisms, the balance of energy in this region is expressed as:

$$Q_m = Q_c + Q_v \qquad (2)$$

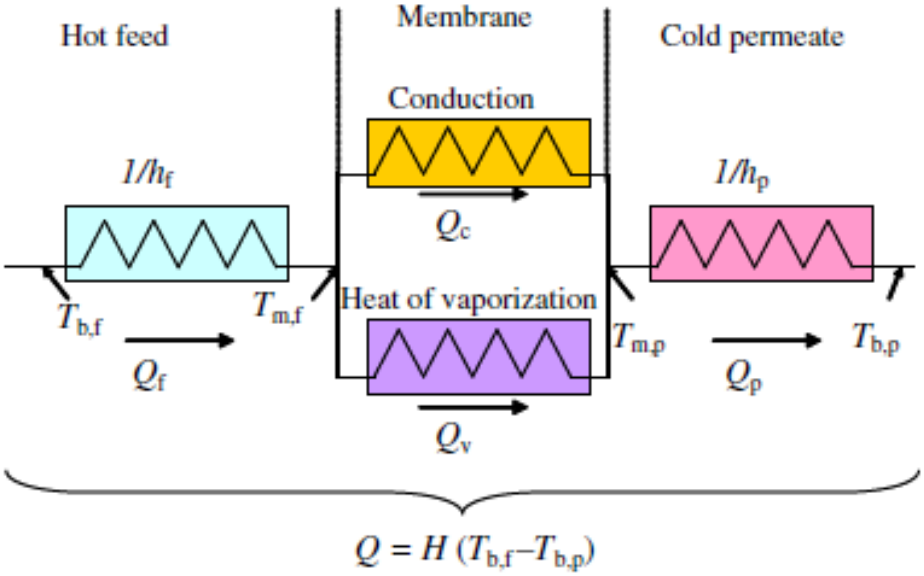

Fig.13. Heat transfer resistances in MD process

The heat transfer due to mass transfer can be written as:

$$Qv = J_w \Delta H_{v,w} \qquad (3)$$

Assuming a linear temperature distribution between the feed- and permeate side membrane surface temperatures T_1 (feed) and T_2, the heat transfer by conduction is given by the following equation:

$$Q_c = \frac{km}{\delta}(T_1 - T_2) \qquad (4)$$

Where *km* is the thermal conductivity of the membrane,

The temperatures in the bulk of the feed- and permeate side medium is different from the corresponding temperatures at the membrane surfaces. This is due to the existence of boundary layers adjacent to the membrane surfaces at both pore ends. Through the feed boundary layer, the convective heat transfer is as follows (Alkhudhiri et al.2012)

$$Q_f = \lambda_f (T_f - T_1) \qquad (5)$$

And in the permeate boundary layer the heat transfer is:

$$Q_p = \lambda_p (T_2 - T_p) \qquad (6)$$

2.7.3. Mass transfer

In the DCMD process, the water vapor is transported from the feed to permeate side due to the difference in chemical potential between both sides of the membrane, which depends on temperature difference, pressure and concentration of the hot and cold flow. Due to the hot feed and the cold permeate counter flow, a temperature difference is induced which creates a water vapor pressure difference, and gives a consequent rise to the transmembrane water vapor flux. The feed solution is the mixture of non-volatile solutes such as salts, colloids and proteins and mostly, the solvent is water. Therefore, water will be the only component which shall undergo the phase change to vapor and passed through the membrane pores. The solution used as feed in this investigation consists of the non-volatile solute salts (225.5gm/lit) dissolved in water.

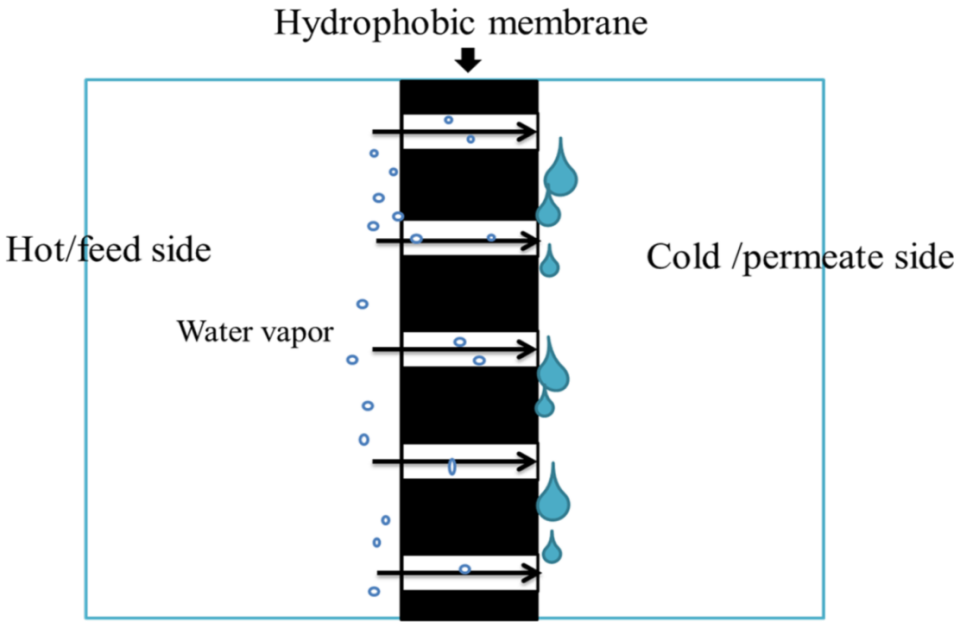

Fig.14. Mass transfer and condensation of vapor in DCMD

Mass transfer occurs in three consecutive steps. At first vapor generates from hot bulk fluid side .Secondly, the generated vapor molecules passes through the porous membrane driving by vapor pressure difference. Thirdly, the vapor molecules come in contact with the cold fluid and condense to water molecule and flows with the cold fluid. Thus, volatile molecules are separated from bulk fluid to permeate fluid. The characteristics of membrane plays very important role for mass transfer of volatile molecules and another controlling factor is vapor pressure driving force. The permeability, thickness of the membrane material, pore size directly influences the mass transfer process as well as rate of mass flux generation. For effective mass transfer the membrane should possess

1. The thickness of the membrane should be in such a way that it reduces the heat transfer efficiency and increases mass transfer permeability.
2. The membrane material should be good enough so that it maintains liquid entry pressure. LEP should be higher than the hydrophobic pressure to overcome pore wetting problems.
3. Thermal conductivity should be low. The conductive heat loss reduces the temperature polarization coefficient which subsequently lowers the mass flux generation.
4. Lower surface energy increases hydrophobicity of the membrane material.

Three basic flow mechanisms govern the mass transfer process of DCMD inside the membrane wall; these are Knudsen diffusion (K), Poiseuille flow (P) and molecular diffusion (M) (Nakoa et al. 2016). These three flow mechanisms occur continuously with in the membrane wall. For Knudsen mechanisms the pore size of the membrane should be very less and the collision between the molecules is negligible in this mechanism. Poiseuille flow occurs when the fluid becomes viscous in nature and the molecule acts as a discontinuous channel in between the membrane pores. And the Molecular diffusion happens when the pore size larger than the free mean path, which is covered by the diffused molecules (Alkhudhiri et al.2012). The Knudsen number (K) is expressed by,

$$K_n = \frac{l}{d} \qquad (7)$$

Where, l=mean free path diffused by the molecule and d=mean pore size of the membrane. Mean free path can be calculated by

$$l = \frac{k_B T}{\sqrt{2}\,\mu P d_e^2} \qquad (8)$$

Where, K_B is the Boltzmann constant (1.380622 ×10−23 J/K), T is the absolute temperature, P is the average pressure inside the polymeric membrane pores. d_e is the collision diameter. Generally the pore size of membrane is ranges in between 0.22 to 1µm and it was estimated that the free mean path is 0.11 µm when feed temperature is 60 ºC. k_n Ranges from 0.11 to 0.55 for 0.22 to 1 µm membranes.

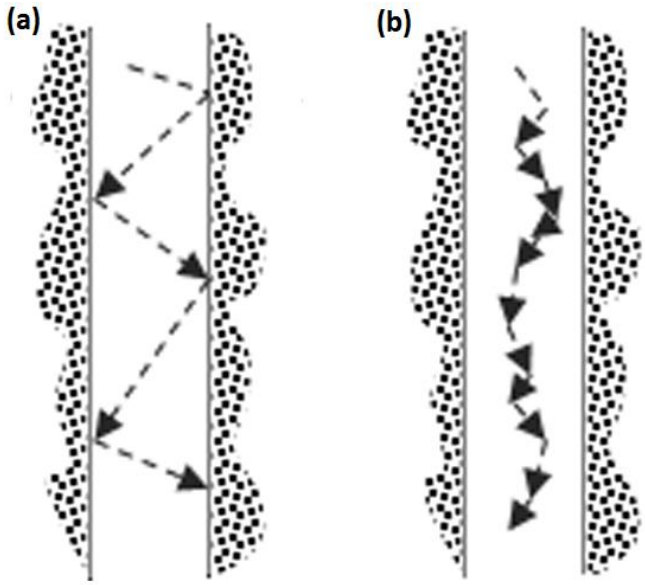

Fig.15. Transport mechanism of (a) Knudsen type of flow and (b) ordinary molecular diffusion type of flow

According to the Fig.12 mass is transferred from hot bulk side to permeate side as a form of vapor by the pressure difference driving force. This mass transfer is also called mass flux which can be calculated by the following expression,

$$J = C_m(P_{1\_}P_2)\ \text{lit}/m^2/\text{hr}. \qquad (9)$$

Where, *J* is the mass flux, Cm is the MD coefficient, and P_1, P_2 are the partial pressures of water vapor evaluated at the membrane surface temperatures T1, T2.
In which,

$$C_m\ \alpha\ \frac{d^a\varepsilon}{tb} \qquad (10)$$

Where α is an exponent coefficient in the range of 1–2. From Equation (10), flux for MD can be increased by increasing pore sizes and porosity and by reducing the tortuosity and thickness of the membrane.

Where, P_1 and P_2 are the partial pressures of water at the feed and permeate sides which can be calculated from Antoine equation shown in Equation 11.

$$P^v = \exp\left(23.328-\left(\frac{3841}{T-45}\right)\right) \qquad (11)$$

Where, P^v is the water vapor pressure in Pa and *T* is the equivalent temperature in K (Qtaishat et al. 2008). It has been observed that an increase in feed temperature results in a significant increase in the mass flux. The use of higher operating temperatures has shown an enhancement in the heat and mass transfer of the DCMD (Yu Hui et al. 2012). However, there is always a threshold for feed temperature because of the liquid entry pressure (or wetting pressure).

2.7.4. Effects of membrane characteristics on DCMD

Different types of synthetic membranes are commercially available in the market. Most commonly used membranes are PP, PTFE and PVDF. Each membrane has different properties such as thickness, pore size, hydrophobicity membrane structure and material characteristics. These properties subsequently affect the process of DCMD. Porosity is one of the major factor responsible for the mass flux or transfer of volatile molecules to the permeate phase. Porosity is the ratio of pore size to the solid surface size of the membrane. Generally, 0.2 to 1 µm pore size membranes are used widely. The increase in pore size also increases the transmission mass flux rate. Membrane thickness is another important factor which is responsible for the mass flux transmission. But its effect is still under investigation. The different membrane material shows various characteristics such as PTFE has highest hydrophobicity than PP and PVDF, thermal and chemical resistivity but it has high conductivity which causes greater heat loss in the DCMD module. PVDF has high thermal stability, less thickness and good hydrophobicity (Camacho et al. 2013). PP also has good thermal and chemical stability but its hydrophobicity is less than others so there should be higher chance of transmission of water molecules instead of water vapor. The rate of permeate mass flux does not depend on the surface area of the membrane but it can significantly lower the specific heat utilization. Moreover, the rate of permeate mass flux increases with increase in feed velocity. Also, enhanced feed temperature increases permeate mass flux. LEP or liquid entry pressure of feed solution should be higher than the hydrophobic pressure so that the vapor which is generated passes instead of the water molecules which can avoid the pore wetting problems.

PVDF membrane shows high surface energy. The contact angle is high for PVDF which is necessary to prevent pore wetting. PVDF membrane exhibits high selectivity but high contact angle has no significant role in permeate flux generation. However, the use of nanoparticles and nanofiber membranes are growing interest in DCMD application

.

Table 3: Reported surface energy and thermal conductivity of most popular materials used in MD

Membrane Material	Surface Energy (×10−3 N/m)	Thermal Conductivity (W m−1 K−1)
PTFE	9–20	~0.25
PP	30.0	~0.17
PVDF	30.3	~0.19

- **Membrane characteristics**

The properties of membranes suitable for membrane distillation should include (Smolders et al. 1989, Zhang et al. 2011):

- A suitable thickness, associated with increased membrane permeability (Tend to increase flux) and decreased thermal resistance (tend to reduce heat efficiency or interface temperature difference) as the membrane becomes thinner;
- Proper distribution of large and narrow pore sizes, so that it can withstand the Liquid Entry Pressure (LEP) of the membrane (Camacho et al. 2013). In MD, the hydrostatic pressure must be lower than the LEP to overcome the membrane wetting obstacle. This can be represented by the Laplace (Cantor) Equation

- LEP= $\frac{-2B\gamma L\cos\theta}{rmax} < P_{process} - P_{pore}$ (12)

Where B is a geometric factor, γl is the surface tension of the solution, θ is the contact angle between the solution and the membrane surface which depends on the hydrophobicity of the membrane, r_{max} is the largest pore size, $P_{process}$ is the liquid pressure on either side of the membrane, and P_{pore} is the air pressure in the membrane pore.

- Membrane should possess low surface energy which means high hydrophobicity.
- Thermal conductivity should be low, which reduces sensible heat transfer and
- High porosity. High porosity increases both the thermal resistance and the permeability of MD

2.7.5. Effect of feed temperature

MD is thermally driven by vapor pressures which vary exponentially with feed temperature. The generated flux is directly influence by the feed temperature. Mainly the heat loss occurs due to the convective heat transfer from hot side to the cold side flow. This heat loss maintains the temperature difference across the membrane. A portion of energy is engaged to generate vapor from water molecules, so the increasing feed temperature also increases vapor generation.

Manawi et al. (2014) had observed the effect of temperature polarization on flux generation. According to the author temperature is a key factor which needs to be considered during the designing of the DCMD experiments. A DCMD model was studied to estimate the temperature polarization coefficient and its effect on local flux generation. In this experimental study the highest temperature polarization was found to be 0.82 when the flow rate was 3 L/min and the feed and permeate temperature were 60 ºC and 20 ºC, respectively. This temperature polarization can be reduced by using turbulence promoters such as spacers.

2.7.6. Parameters for temperature polarization reduction

For maximum flux generation vapor pressure difference should be high to reduce the temperature polarization effect (Camacho et al. 2013). Therefore, the convective heat transfer coefficient should be high for better flux generation. This convective heat transfer coefficient is expressed by the following equation

$$\alpha_f = -\frac{\lambda_f}{T_{f-T_1}} \left(\frac{dT}{dY}\right)_{boundary} \qquad (13)$$

Where, λ_f is thermal conductivity of the feed, $\left(\frac{dT}{dY}\right)_{boundary}$ is the temperature gradient in the thermal boundary layer of the feed side. From the above equation, the convective heat coefficient can be improved by reducing the thermal boundary layer of the feed side. This thermal boundary layer can be reduced by creating turbulence in the feed steam flow, which will also improve the permeate flux generation.

The turbulence can be promoted by using net like spacer or zigzag spacer, shown in the Fig.17.These spacers can reduce the thickness of boundary layer and improve the α_f. However, the hydrodynamic pressure reduces the effect of spacers.

2.7.7. Membrane Fouling and Wetting

Membrane fouling is one of serious obstacle in the application of membrane technologies (Schafer et al. 2005, Scott et al.1995) as it causes flux reduction. The fouling is the deposition of organic and inorganic matter in the pores of the membrane, which reduces the permeability of a membrane. Although the DCMD is more resistive to fouling than conventional membrane technologies such as RO, UF Dow et al. (2005) studied that lower feed temperatures can substantially reduce the risk of fouling in DCMD.

The hydrophobic membrane is the separating barrier between the feed and permeate flow, membrane wetting is the flowing of non-volatiles molecules across the membrane. Membrane wetting can occur under the following conditions:

• When the hydraulic pressure on the surface of the membrane is greater than the liquid entry pressure (LEP).
• The clogging by solute particles on the membrane surface can effectively reduce the hydrophobicity of the membrane property (Gryta et al. 2005), which was generally observed in a long-term operation for high-concentration feeds such as for brine crystallization.
• High organic content or presence of surfactant substances in the feed lowers the surface tension of feed solution which reduces the hydrophobicity of the membrane via adsorption and lead to membrane wetting.

2.8. Recent DCMD models

Different models on DCMD have been developed by researchers to improve the process parameters for better understanding of the fundamentals of DCMD. A model was established by Zhang et al. particularly for PTFE membrane on the basis of its high compressibility, thickness and pore size (Zhang et al. 2012) to predict flux and evaporation ratio. Assuming that tortuosity remains constant during membrane compression. This model is applicable at higher temperatures so that there will be a great variation in membrane compression property. It was noticed that the pressure drop could be restricted by reducing the membrane length and using of compressible membranes. In a study carried out by Martinez et al. (2002), it was observed that for narrow pore size distributions in commercial membranes molecular and Knudsen diffusions play significant role in mass transfer when the stagnant air is present in the module, whereas in the absence of stagnant air, viscous and Knudsen contributions are important. But, for membranes with smaller pores at low temperatures, low vapor pressure difference, the viscous contribution is very less. Some of the recently developed models regarding DCMD technology are black box, grey box, and two dimensional models.

2.8.1. Black box models

A study was conducted by Rao et al. (2014) using a simplified flux prediction method for DCMD modelling considering membrane structure is a significant parameter. They also claimed that many of the complex models for DCMD are based on unreliable mass transfer assumptions. He established the relationship between 18 different structural membrane parameters and permeates flux. Several parameters (ε (porosity)/δ (thickness), ε/τδ, 1/τδ, and a new parameter introduced by them i.e. coupled membrane structural property or Cm) were observed to improve the permeate flux. Cm was developed in such a manner so, that it is simple and not costly to measure. Predictions that were assumed in this model are more accurate than the dusty gas model (DGM). Moreover; Bosanquet's assumption has been combined with Knudsen and Brownian diffusion to investigate the fundamental aspects of heat and mass transfer in DCMD (Kim et al. 2013). Theoretical studies have been conducted with software or computational application, the solution of Fick's law was carried out in its original differential form in this study to obtain the molar flux of water vapor through a DCMD membrane pore. An effective diffusion coefficient was obtained from the combination of Knudsen and Brownian diffusion coefficients. The results which were obtained, showed that increase in vapor also increase the heat flux through membrane pores and the theoretical prediction of permeate flux supports the experimental observations reported in the literature.

2.8.2. Grey-Box model

Grey –box model is another type of modelling that has been introduced to investigate the fundamental DCMD performance based on some parameters in DGM. There three types of DGM have been established to evaluate heat and mass transfer performance in DCMD. Some experiments were carried out by Jensen et al. using deionized water and aqueous salt solutions of NaCl with concentration levels up to 15 ppm as feed to find the parameters for effective heat and mass transfer. The results showed that Knudsen molecular diffusion transition model yielded the best prediction for heat and mass transfer. In addition, the most accurate heat transfer correlations were found to be the Lévêque equation and the Dittus–Boelter equation for laminar flow and turbulent flow, respectively.

Response surface methodology (RSM) model has also been established to find out DCMD processes. Boubakri et al. (2014) has developed a model to optimize the operating parameters which affecting water desalination in DCMD using RSM. Manawi et al. (2014) studied the operational parameters which effects the distillate flux generation in DCMD. The effect of temperature polarization has also been observed for desalination of high salinity feed. This model showed that flux can be improved by maintaining counter-current flow and using of spacers. The model also said that temperature polarization effect reduced the flux due to the deposition of solute particle on the membrane surface causing a temperature difference in between bulk liquid and the membrane interface. This could be arrested by high flows and using of spacers.

2.8.3. Two-dimensional dynamic model

Most of the DCMD models are one dimensional steady state system where empirical equations were applied. Recently two-dimensional system has been established by Bin Ashoor et al. (2016) for DCMD in plate-frame configuration. This mathematical model obtains the temperature and concentration distribution in both and cold fluid channels and also local flux generation in the membrane surface. The model predicts the simultaneous energy and mass balances, which are important for analysis, design and optimization of DCMD.

2.9. Applications of DCMD

DCMD has been introduced in different purposes like desalination of sea water, wastewater treatment, ground water purification, removing of heavy metals and micro pollutants from water. DCMD has also been introduced in food industries for juice concentration, preparation of condensed milk. Nowadays, DCMD has been widely used for treating produced water, pharmaceutical waste stream and radioactive wastewater. The treatment of wastewater has become a prime focus for sustainability of water so that it can be reused.

2.9.1. Produced water treatment

A huge amount of oily waste water is being produced by petroleum based industries and oil refineries. This oily wastewater has an adverse impact on marine ecosystem. Produced water is the byproduct produced along with gas and oil from refineries and petroleum industries. This water also contains dissolved organic solvents, toxic metals and radioactive elements which are the main concern for the environment. There are three main sources from where produced water is being generated (1) water injected into the reservoir to enhance oil recovery, (2) flow back water from hydraulic fracturing activities, and (3) a mixture of both. This causes surface water pollution associated with the groundwater contamination.

In past, physical, chemical and biological treatments were used for treatment of produced water effluents. The physical method removed the suspended solid particles and chemicals like activated carbon, zeolite were used for absorption of carbon. Sand filters were also used to remove suspended metal particles. The chemical treatment associated with the removal of dissolved and colloidal substances by extraction, precipitation, ozone treatment. For biological treatment different aerobic and anaerobic processes are employed to remove dissolved organic and inorganic loads. However, these processes suffer from disadvantages like high treatment cost, usage of hazardous chemical substances which has a further impact on living organisms. So these drawback leads to the introduction of membrane technology for treatment of produced water. DCMD offers 70% recovery for produced water.

2.9.2. Application in food industry

DCMD has been successfully introduced in food industries for juice concentration as well as for waster effluent treatment. An experimental study was carried out by Jensen et al. (2011) to concentrate black current juice. A theoretical DCMD model has been developed. The concentration polarization in the membrane surface was estimated by empirical correlation with heat and mass transfer coefficients. DCMD has been also used for apple juice concentration and it showed 50% recovery of its initial concentration. The permeate flux was achieved 9kg/m^2h. PTFE membrane was applied for this process and the processing parameters were studied. DCMD has also been introduced in the Dairy industry to concentrate whole milk, skim milk and whey products. This study was performed in Australia by flat sheet PTFE membrane and the generated flux was obtained 10 kg/m^2h.

2.9.3. Chemical treatment

DCMD has also been incorporated in chemical industries to produced different chemicals associated with several chemical treatments. KCl was converted to $KHSO_4$ (Tomaszewska et al. 2012) by DCMD when the hot inlet feed temperature were 333 to 343 K and for permeating side it was 293K. Concentration of pure HCl was achieved by 43gm/dm^3. DCMD can remove heavy metals by using of hybrid PTFE membrane. Toxic chromium was

removed from simulated water by Bhattacharya et al. using different membranes. The results showed that the hydrophobic PTFE membrane coupled with polyethyleneterephthalate (PET) achieved improved performance in terms of normalized flux. Qu et al. (2013) carried out an investigation to remove ammonia from aqueous solution. This study was done by DCMD, modified DCMD and a hollow fiber membrane contractor (HFMC), and the results showed that the removal for three different set –up were 52 %, 88% and 99.5% within 105 minutes respectively. Arsenic was also removed by solar driven DCMD with hydrophobic flat sheet membrane made up of PP, PTFE. Fluoride present in ground water has been removed by PVDF membranes. For this study permeate flux was obtained 35.6 kg/m^2h.

Chapter 3

Materials and Experimental procedure

Chapter 3

3. Materials and Experimental procedure

3.1. DCMD set-up

The DCMD set-up is consist of three main parts; membrane module, hot saline reservoir and the chiller (Fig 16). The main functional part is the membrane module section which is a polymethylmethacrylate (PMMA) membrane cells fitted with flat sheet membranes. The module section is divided horizontally into two halves and produced two narrow chambers. The internal dimension of each chamber is 30 cm long, 15 cm wide and 4.5cm deep. The active surface area for heat and mass transfer are 0.045 m^2. The chambers are separated horizontally by the thin polymeric membrane. Each side of the membrane was supported by spacer to enhance turbulence. Rubber gaskets, approximately 5 mm in width, on each side of the membrane guaranteed secure mount of the membrane. The whole system was a closed-loop bench scale set up where hot flow and the cold flow were maintained in a counter-current direction. The flowrate was 100 lit/hour for both hot and cold flow.

Fig.16. DCMD equipment used in this study (1) heater and reservoir for hot side feed (2) heater and reservoir for reheating of cool brine reject (3) temperature controller for hot side feed and hot pump regulator (4) temperature controller for reheating (5) Hot feed pump (6) DCMD module (7) Hot side feed flow meter (8) Cold side flow meter (9) Cold side pump (10) Cold pump regulator (11) Cold side temperature controller and chiller

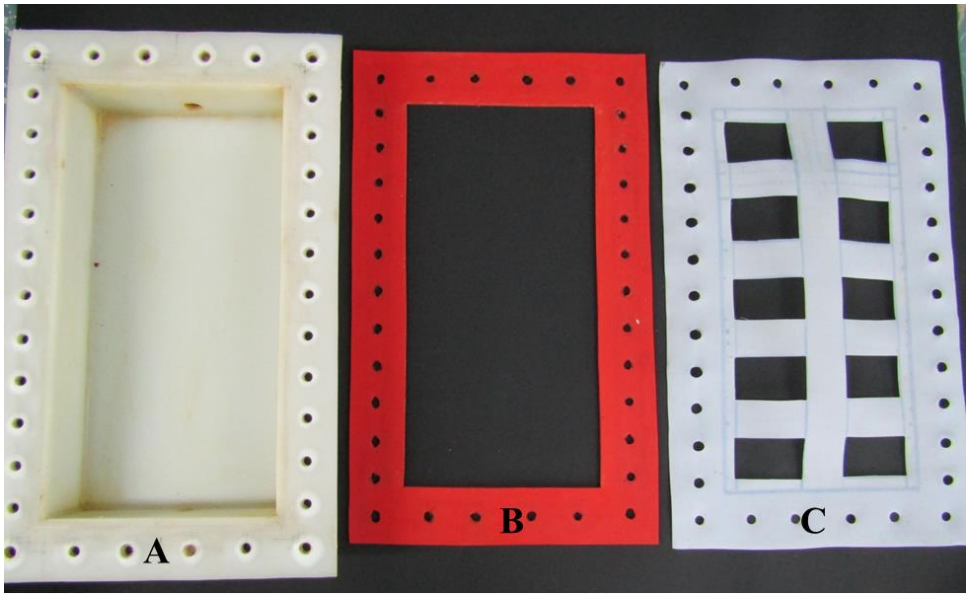

Fig.17. Components of the DCMD module (A) flow chamber of DCMD (B) rubber gasket (C) Teflon turbulence enhancing spacer

3.2 Membranes

Three different types of synthetic membranes of various pore sizes were applied to optimize each membrane's efficiency in diverse operational condition. The membranes are Polypropylene (PP), Polytetrafluorethylene (PTFE), Polyvinylidene difluoride (PVDF), manufactured by Tisch Environmental Inc., Ohio, United States.. Each membrane has three different pore sizes of 0.22µm, 0.45µm and 1µm. The thickness of the PP and PTFE membranes were 0.20±0.1 mm, while that of the PVDF membranes were 0.085-0.12 mm as per the manufacturer's specifications. A new membrane was used for each experiment.

Table 4: List of membranes used

Sl. No	Membranes	Pore size(µm)
1	Hydrophobic PVDF roll membrane(RS20233)	0.22
2	PVDF filter membrane(RS20433)	0.45
3	Hydrophobic PVDF membrane(RS20133)	1
4	PTFE membrane roll stock(RS40213)	0.22
5	PTFE membrane roll stock(RS40413)	0.45
6	PTFE roll membrane stock (RS40113)	1
7	PP roll membrane	0.22
8	PP membrane roll stock(RS30423)	0.45
9	PP membrane roll stock(RS30123)	1

3.3. Composition of the feed solution

Synthetic feed MST media was prepared following the same composition for bioplastic production to maintain the high salinity. The composition is NaCl 200.0; $MgSO_4.7H_2O$ 20.0 (g/lit); KCl 2.0 (g/lit); $C_5H_8NNaO_4$ 1.0 (g/lit); KH_2PO_4 0.0375 (g/lit); $FeSO_4.7H_2O$ 0.05 (g/lit); yeast extract 1.0 (g/lit). For each set of operation 5 liters of feed solution was prepared according to this composition.

3.4. Procedure

3.4.1. Installation of the DCMD set-up

The installation of the set –up was one of the important parts of this investigation. Different components were fabricated by local manufacturer. Therefore, several experimental trial runs were taken to install the set-up properly. Initially, heat resistive autoclavable plastic sheets were applied instead of membranes to separate the hot and cold flows. Once the set –up was responded correctly, the counter-current direction of both hot and cold flow was checked. Leakage tests were done to ascertain the proper functioning of the DCMD module. Chemical dye was used to check the cross mixing of the hot and cold fluid in between the module of the DCMD. Finally the hot side and the cold side temperature were set to check the PID controllers of both hot and cold side were properly functioning or not.

3.4.2. Experimental procedure

In this project work, two types of experiments were conducted for the optimization of DCMD performance. In the first few experiments the MD equipment was performed with its simpler form (without reheating). In this case, reasonable flux could not obtain so; the set-up was modified with a secondary heating coil.

- **Phases of the work**

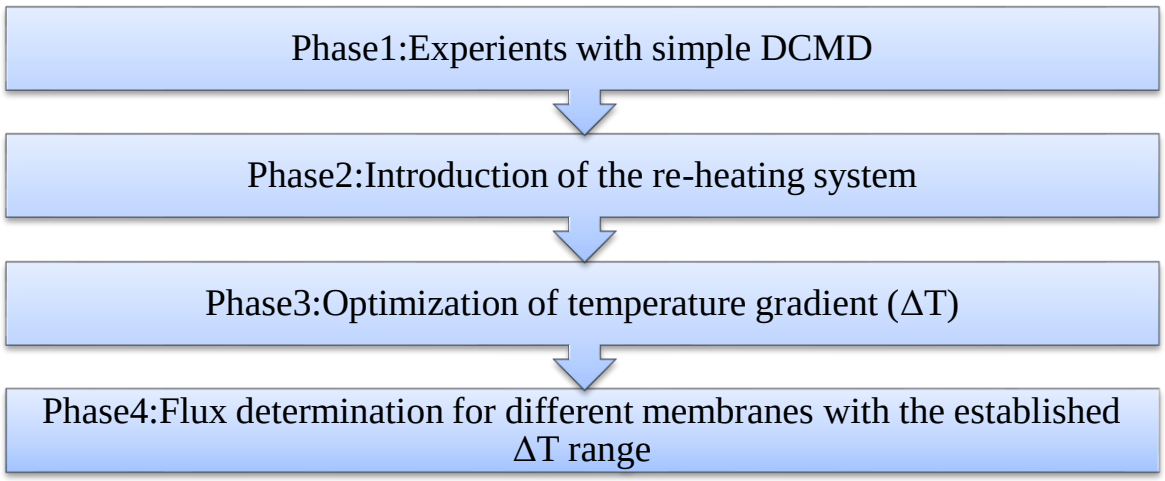

3.4.2.1 Experiment with simple DCMD (without reheating)

The performance of traditional DCMD set up was optimized under different operational conditions. The tests were performed using PP and PTFE membranes of pore size 0.22µm and 0.45µm with varying temperature range. The highly saline feed solution (20w/v) was pre heated by thermostatic heater and continuously pumped to the bottom section of the module by a centrifugal pump. Simultaneously, permeate water was cooled down by a chilling system and pumped in counter-current direction to the upper part of the module. Both, the flows were separated by the membrane, where the mass and heat transfer occurred continuously from hot side to the cold side. Pressure gauges were attached in the inlet and outlet of both hot and cold channels. Whereas, the hot inlet pressure gauge showed overall 5 psi deflection but the outlet gauges did not show any deflection. The effective mass and heat transfer membrane area was $0.045m^2$.The separated permeate water mixed with the cold channel and flowed back to the chilling system and the concentrated feed solution returned to the primary reservoir. Hence, whole system acted as a closed system and the experiment was run until the feed saline solution become viscous (maximum 5 hours)

Five experimental runs were carried out in different temperature range to find out the best operational temperature range for maximum flux generation. The temperature of feed and permeate solution were maintained ± 5 ºC of the set value and controlled by PID controller. However, the feed side temperature is varied from 70 to 90 ºC and cooling temperature was maintained at 5 to 15 ºC. Every 30 minutes interval feed sample was drawn from feed for TDS measurement. 5 ml of each sample were dried in the hot air oven drier at 90 to 100 ºC. From these TDS values the permeate fluxes were calculated.

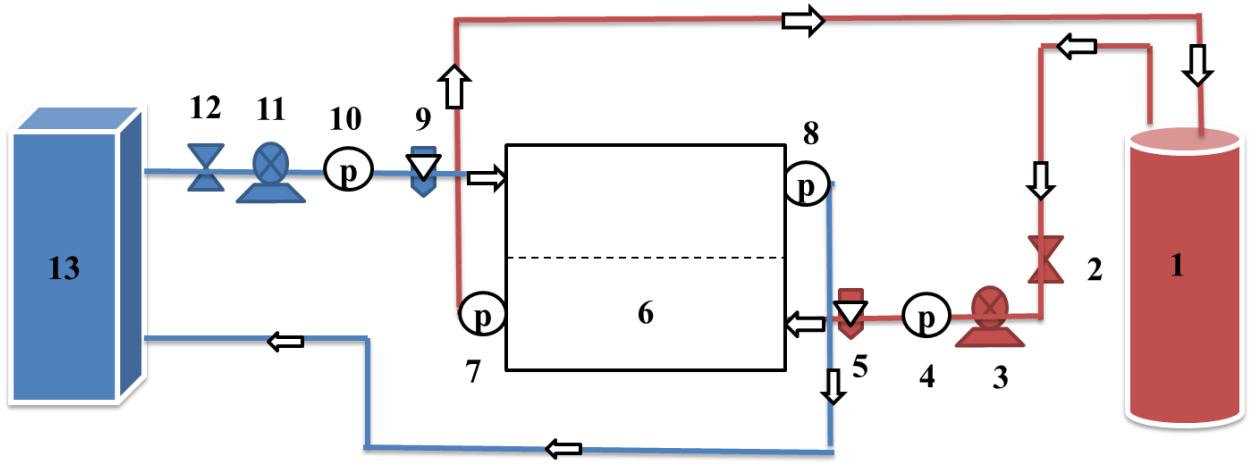

Fig.18. Schematic of simple DCMD (without reheating) (1) heater and reservoir for hot side (2) hot inlet valve (3) hot side pump (4) hot intel pressure gauge (5) hot side flowmeter (6) DCMD module (7) hot outlet pressure gauge (8) cold outlet pressure gauge (9) cold side flowmeter (10) cold inlet pressure gauge (11) cold pump (12) cold inlet valve (13) chiller

- **Flow chart of one single run**

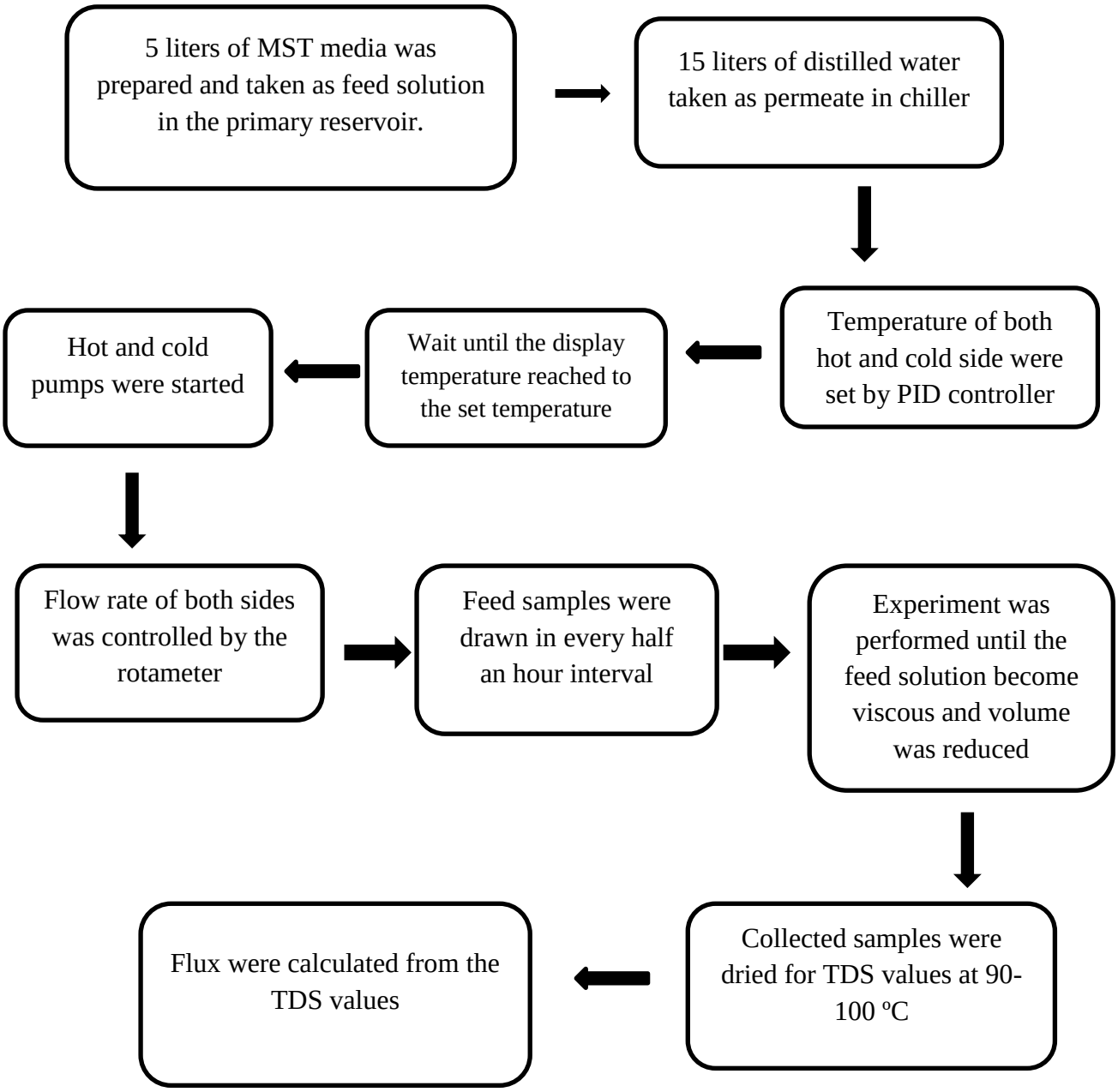

3.4.2.2. Modified DCMD set –up

Reasonable flux (of water from hot to cold side) was not obtained in the previous experiments and hence the separation of salts from water could not be attained. The reason for the poor flux was the rapid decline of the hot side temperature during its passage against the cold stream. This can be maintained by reheating the cool saline solution repeatedly. So, in the experiments described now a secondary heating source was introduced at the hot side

exit so the heat loss of the hot stream was compensated. In this way the hot side temperature remained constant and a stable ΔT was maintained. This phenomenon can be expressed by the following equation:

$$F = (1-t)\frac{C_P(T_F - T_E)}{\Delta H_{Vap}} \qquad (14)$$

Where, T_F and T_E are the feed and exit temperatures CP is the specific heat of water (4.18kJ/kg/K), t is the proportion of conductive heat loss through the membrane, and $\Delta Hvap$ is the latent heat of vaporization (kJ/kg).

To overcome this reduction in temperature (ΔT), certain modification was done in the traditional DCMD set up. Previously, the outlet hot solution (lower in temperature due to the rapid heat transfer) returned to the primary vessel, from where the inlet solution to the DCMD flowed (showed in Fig 2). After the modification, the outlet flow which was coming from the hot side of the module was collected separately in a stainless steel buffer container and heated up by an induction coil heating system (showed in Fig 19). Then the heated solution was flowed to the primary vessel. This modification maintained the desired ΔT for the effective mass transfer process of DCMD.

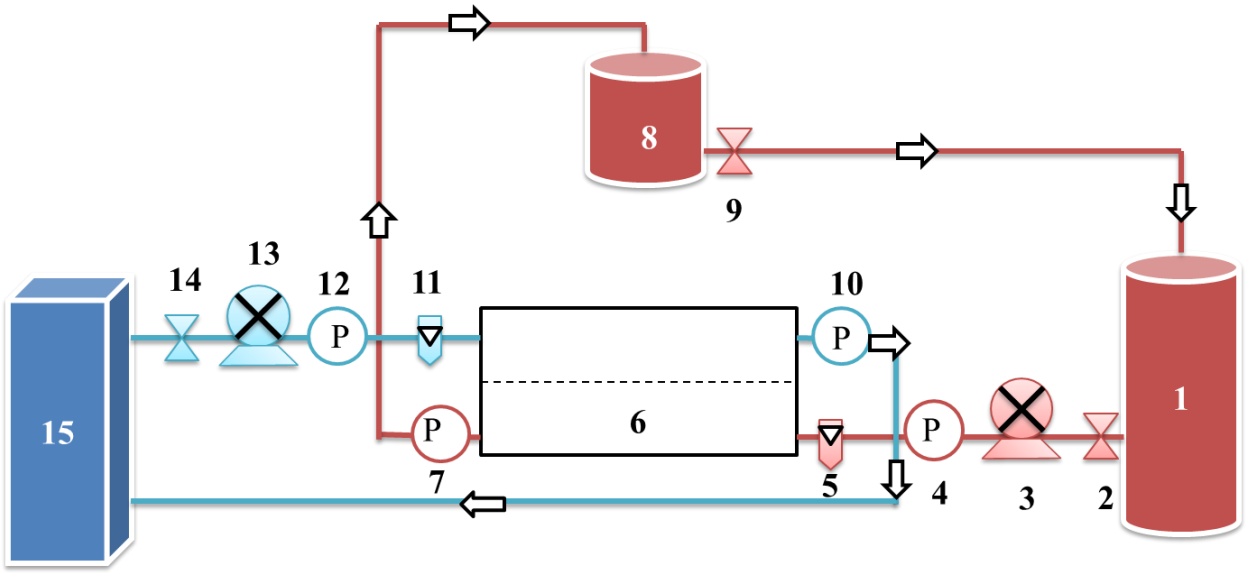

Fig.19. Schematic of modified DCMD process (1) heater and reservoir for hot side (2) hot inlet valve (3) hot side pump (4) hot intel pressure gauge (5) hot side flowmeter (6) DCMD module (7) hot outlet pressure gauge (8) hot reheating tank (9) reheating tank valve (10) cold outlet pressure gauge (11) cold side flowmeter (12) cold inlet pressure gauge (13) cold pump (14) cold inlet valve (15) chiller

Fig.20. DCMD Reheating equipment (1) heater and reservoir for hot side feed (2) inductive heating system (3) reservoir for cool brine reject.

3.5. Experiment for observing evaporation

Some portion of the saline hot solution was evaporated in the ambient environment from the primary vessel when the ΔT in above 85ºC. Such evaporative loss increases the concentration of saline feed solution. This effect altered the mass and heat transfer efficiency of DCMD. Moreover, the evaporation reduces the temperature gradient as a result the mass transfer in DCMD reduced. To check such evaporative loss an experimental run was conducted so that the percentage of the evaporation can be calculated. As per previous run 5 liters of saline solution (20w/v) was prepared and heated up by thermostatic heating system. The solution was heated for 5 hours (time taken for crystallization of salts) and 85ºC was maintained throughout the run. Final volume was collected 4.75 liters.

3.6. TDS measurement

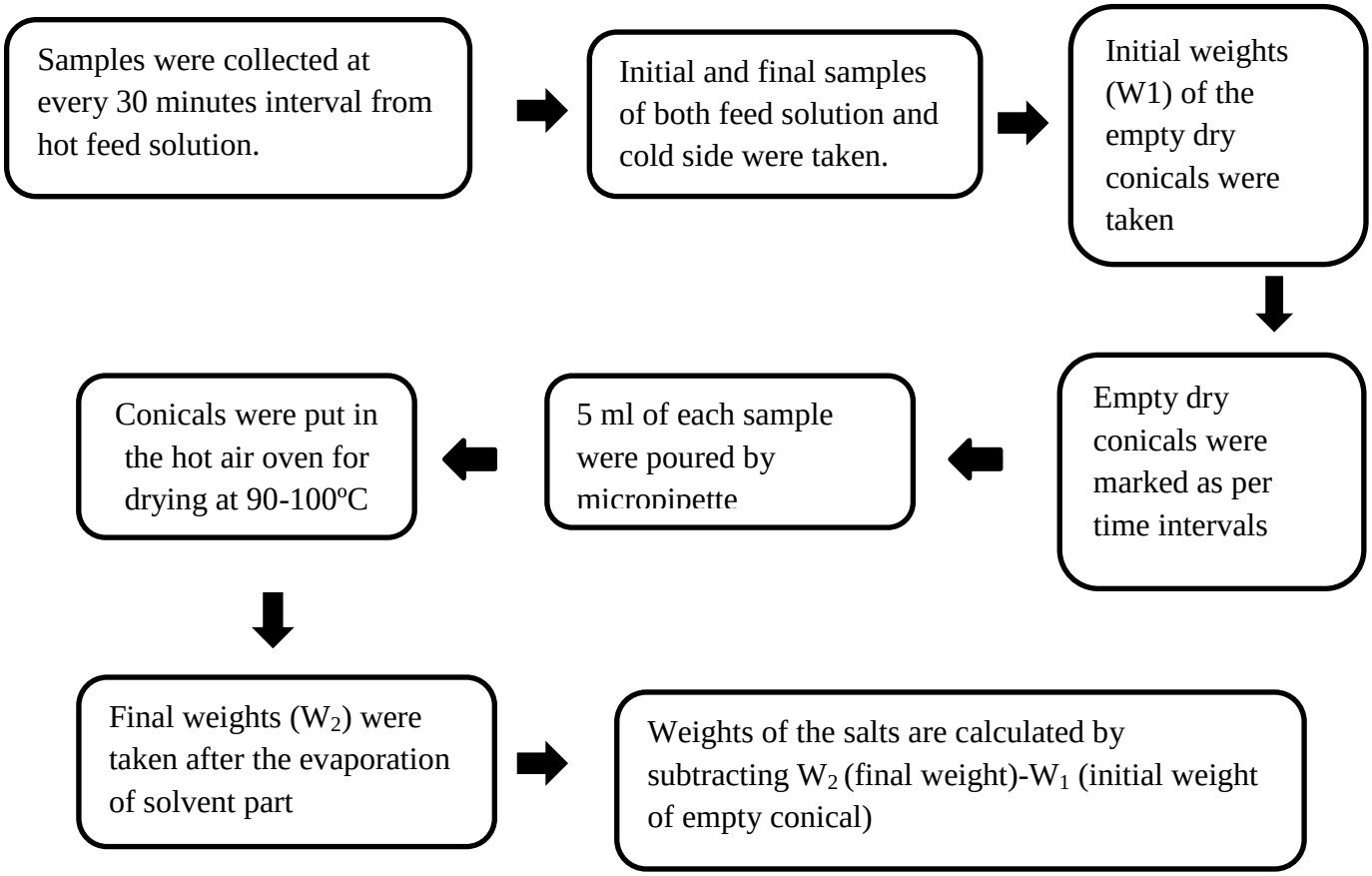

3.7. List of experiments

Table 5: Without reheating of cool brine reject with simple DCMD

Membrane	Pore size (µm)	Hot side temp(ºC)	Cold side temp(ºC)	ΔT (ºC)
PP	0.22	75	5	38-66
PP	0.45	70	5	42-62
PP	0.22	90	15	36-76
PTFE	0.22	70	5	37-61
PTFE	0.22	90	5	36-83

Table 6: Reheating of cool brine reject with modified DCMD

Membranes	Pore size (µm)	Hot side temp.(ºC)	Cold side temp.(ºC)	ΔT (ºC)
PP	1	85	20	54-65
PP	0.45	85	20	62-65
PP	0.22	85	20	63-67
PTFE	1	85	20	62-65
PTFE	0.45	85	20	61-65
PTFE	0.22	90	5	83-86
PTFE	0.22	70	5	63-67
PTFE	0.22	85	20	60-67
PVDF	1	85	20	57-65
PVDF	0.45	85	20	60-67
PVDF	0.22	85	20	63-65
PVDF	0.22	80	25	52-57
PVDF	0.22	75	20	49-54

Chapter 4
Observation and Results

Chapter 4

4. Observation and Results

➢ *Phase1: Experiments with simple DCMD*

4.1. Experiment with 0.45µm PP at ΔT 65ºC

Table 7: Temperature gradient and total dissolved solid (TDS) for hot side temperature (70 ºC) and cold side temperature (5 ºC)

Time (hr.)	Hot side temp.(ºC)	Cold side temp.(ºC)	ΔT(ºC)	TDS (gm/lit)
0	65	3	62	172.04
0.5	48	4	44	173.56
1	49	7	42	178.42
1.5	50	6	44	186.88
2	51	6	45	183.42
2.5	51	8	43	188.12
3	49	7	42	190.42
3.5	50	6	44	198.46
4	50	9	46	209.44

Table 8: Generated flux with respect to time (0.5 hr.)

Time (hr.)	Flux (lit/m^2hr.)
0.5	1.94
1	3.97
1.5	5.88
2	3.44
2.5	3.79
3	3.57
3.5	4.22
4	4.96

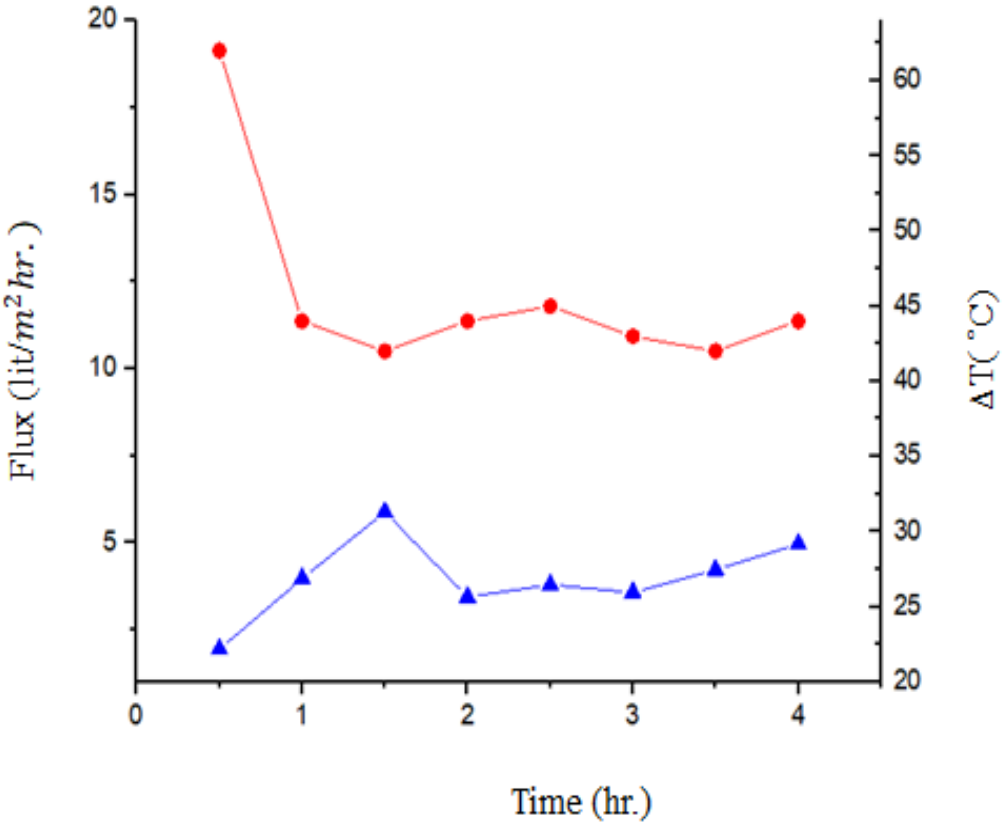

Fig.21. Graphical representation of flux for 0.45 µm PP with respect to time and temperature gradient (42 ºC to 62 ºC).Where Red color indicates the temperature gradient and blue color indicates the flux.

➢ Observation

Salts were found in permeate (cold) side. Rapid decline in feed temperature (65 to 42 ºC) was observed during its passage against the cold flow thus poor flux was generated. Crystallization did not occur after 3 hours.

4.2. Experiment with 0.22µm PP at ΔT 65ºC

Table 9: Temperature gradient and total dissolved solid (TDS) for hot side temperature (75 ºC) and cold side temperature (5 ºC)

Time (hr.)	Hot side temp.(ºC)	Cold side temp.(ºC)	ΔT(ºC)	TDS(gm/lit)
0	72	6	66	208.56
0.5	52	7	45	222.52
1	48	6	42	222.46
1.5	48	8	40	219.02
2	46	6	40	228.16
2.5	45	7	38	235.36
3	45	7	38	232.22
3.5	46	7	40	238.84
4	48	7	39	239.32
4.5	49	7	42	254.8
5	49	8	41	287.22

Table 10: Generated flux with respect to time (0.5 hr.)

Time (hr.)	Flux (lit/m^2hr.)
0.5	13.9413
1	6.9425
1.5	3.5376
2	4.7724
2.5	5.0608
3	2.8913
3.5	2.8133
4	2.5146
4.5	4.4808
5	6.0859

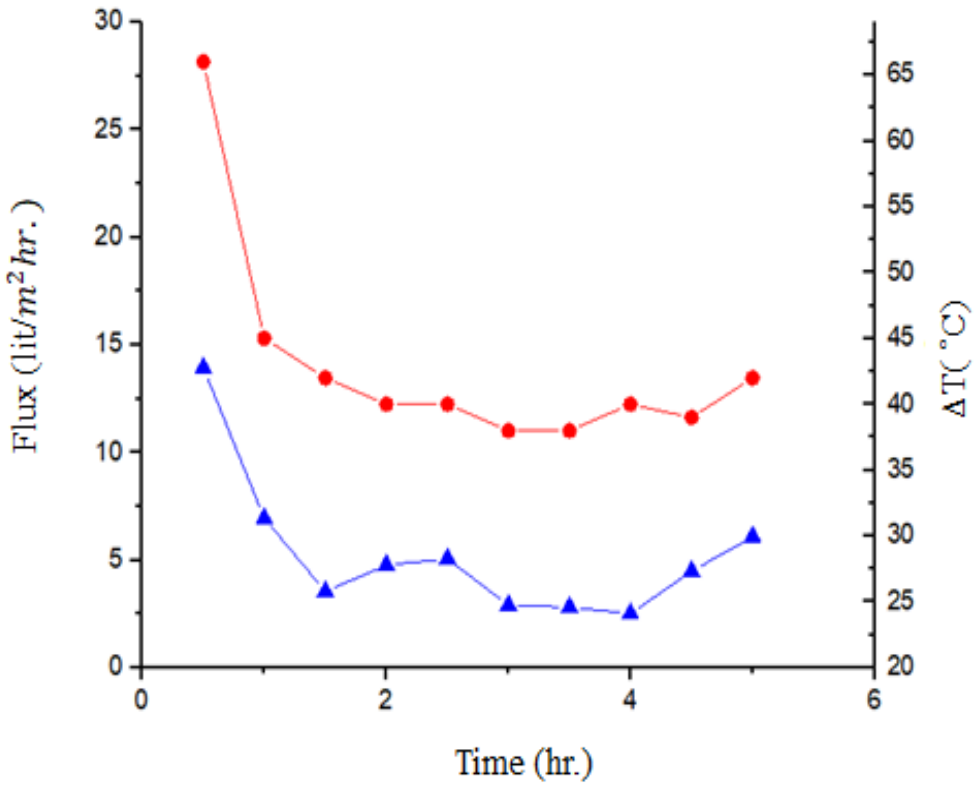

Temperature gradient (º C)
Flux (lit/m^2hr.)

Fig.22. Graphical representation of flux for 0.22 µm PP with respect to time and temperature gradient (38 ºC to 66 ºC).Where Red color indicates the temperature gradient and blue color indicates the flux.

➢ Observation

Salts were found in the permeate side after the experiment. The initial flux was high but declined very rapidly as the temperature of feed solution was reduced suddenly after the Expt. has started. Crystallization did not occur after 5 hours of Expt.

4.3. Experiment with 0.22µm PP at ΔT 75ºC

Table 11: Temperature gradient and total dissolved solid (TDS) for hot side temperature (90 ºC) and cold side temperature (15 ºC)

Time (hr.)	Hot side temp.(ºC)	Cold side temp.(ºC)	ΔT(ºC)	TDS (gm/lit)
0	90	14	76	207.14
0.5	57	18	39	228.06
1	56	17	39	221.38
1.5	53	17	36	246.4
2	54	15	39	231.02
2.5	55	16	39	234.4
3	53	17	36	237.82
3.5	54	16	38	244.44
4	54	17	37	247.638
4.5	57	16	39	253.72
5	59	17	42	262.76

Table 12: Generated flux with respect to time (0.5 hr.)

Time (hr.)	Flux (lit/m^2hr.)
0.5	20.38
1	7.14
1.5	11.8
2	5.74
2.5	5.16
3	4.77
3.5	3.69
4	1.339
4.5	4.53
5	4.70

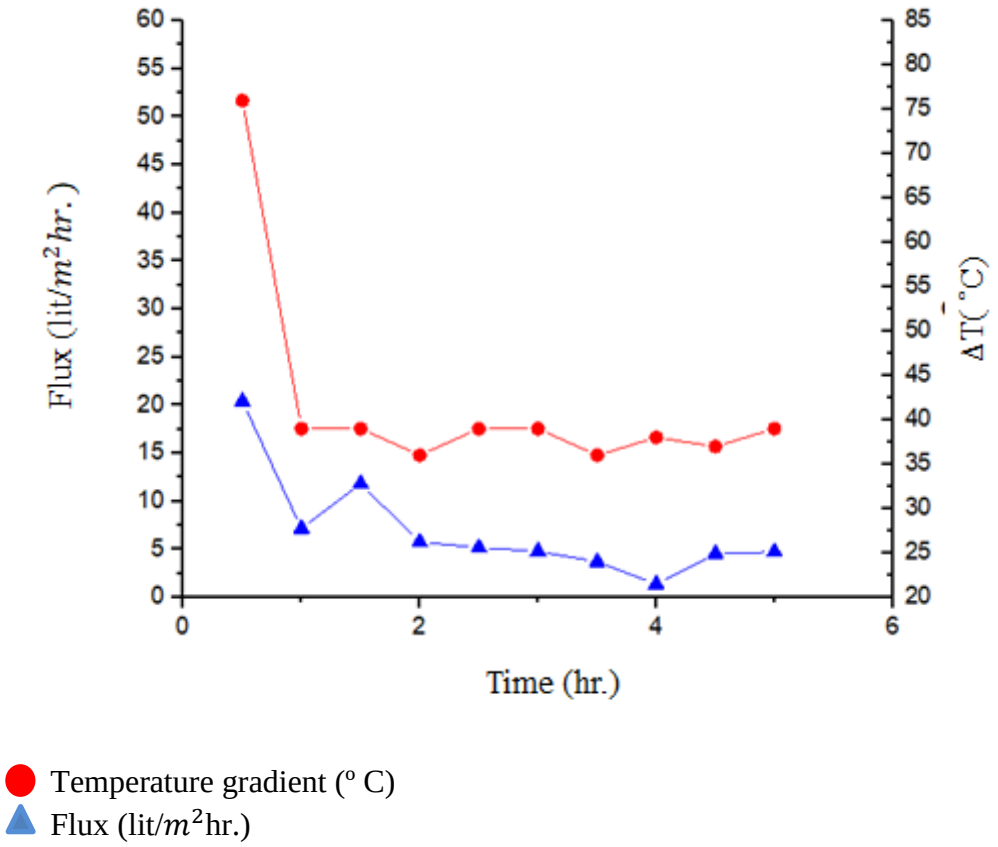

Fig.23. Graphical representation of flux for 0.22 µm PP with respect to time and temperature gradient (36 ºC to 76 ºC).Where Red color indicates the temperature gradient and blue color indicates the flux.

➢ Observation

The overall flux was poor with rapid declination as the temperature gradient (ΔT) was not steady throughout the Expt. Salts were absent in the cold side. Crystallization did not occur after 5 hours of Expt.

4.4. Experiment with 0.22µm PTFE at ΔT 65ºC

Table 13: Temperature gradient and total dissolved solid (TDS) for hot side temperature (70 ºC) and cold side temperature (5 ºC)

Time (hr.)	Hot side temp.(ºC)	Cold side temp.(ºC)	ΔT(ºC)	TDS(gm/lit)
0	67	6	61	211.62
0.5	48	6	42	214.06
1	45	5	40	236.42
1.5	43	6	37	212.8
2	43	6	37	216.18
2.5	43	6	38	223.58
3	44	5	40	214.48
3.5	45	7	39	232.12
4	46	5	42	233.72
4.5	47	6	41	239.7
5	47	5	42	239.82

Table 14: Generated flux with respect to time (0.5 hr.)

Time (hr.)	Flux (lit/m^2hr.)
0.5	2.53
1	11.6721
1.5	2.4107
2	1.1718
2.5	2.3774
3	2.4938
3.5	2.8036
4	2.6265
4.5	2.8925
5	2.613

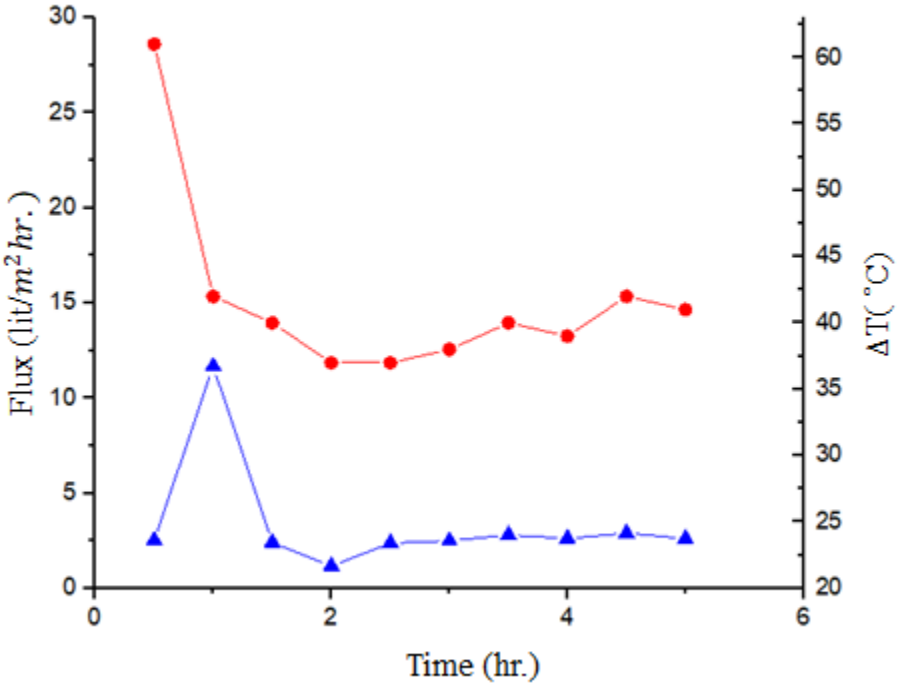

Fig.24. Graphical representation of flux for 0.22 µm PTFE with respect to time and temperature gradient (37 ºC to 61 ºC).Where Red color indicates the temperature gradient and blue color indicates the flux.

➢ Observation

Salts were not found in the permeate side. Initial flux was very high but the average flux was poor as the ΔT was reduced as soon as the Expt. starts. Crystallization of salts was not observed after 5 hours of experiment.

4.5.Experiment with 0.22 PTFE at ΔT 85ºC

Table 15: Temperature gradient and total dissolved solid (TDS) for hot side temperature (90 ºC) and cold side temperature (5 ºC)

Time (hr.)	Hot side temp.(ºC)	Cold side temp.(ºC)	ΔT(ºC)	TDS (gm/lit)
0	90	7	83	193
0.5	49	7	42	205.24
1	46	6	40	227.84
1.5	46	6	40	237.52
2	46	6	40	238.3
2.5	46	6	39	258.72
3	45	7	39	250.42
3.5	46	6	40	250.5
4	45	6	39	263.42
4.5	44	6	38	254.56
5	42	6	36	259.34

Table 16: Generated flux with respect to time (0.5 hr.)

Time (hr.)	Flux (lit/m^2hr.)
0.5	13.2527
1	16.99
1.5	13.88
2	10.56
2.5	11.2897
3	8.4923
3.5	7.287
4	7.4258
4.5	5.971
5	5.6845

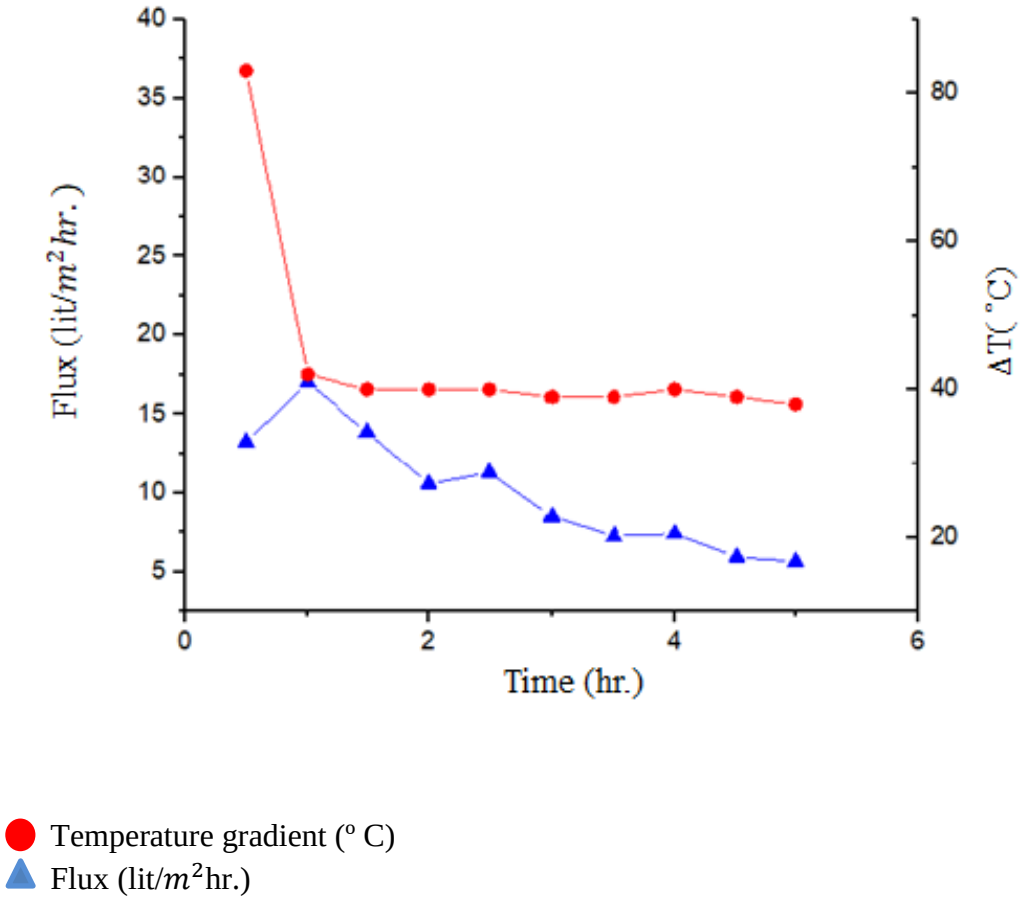

Fig.25. Graphical representation of flux for 0.22 µm PTFE with respect to time and temperature gradient (36 ºC to 83ºC).Where Red color indicates the temperature gradient and blue color indicates the flux.

➢ Observation

Salts were absent in the permeate side. Flux was decreased with decline in temperature gradient (36ºC to 83ºC).As the ΔT was high better flux obtainer as compare to Expt.#4.4.Crystallization did not occur (after 5 hours).

- ***Phase 2: Introduction of the re-heating system***

4.6. Experiment with 0.22µm PTFE at ΔT 85ºC

Table 17: Temperature gradient and total dissolved solid (TDS) for hot side temperature (90 ºC) and cold side temperature (5 ºC)

Time(hr.)	Hot side temp.(ºC)	Cold side temp.(ºC)	ΔT(˚C)	TDS(gm/l)
0	90	4	86	243.84
0.5	84	4	80	269.66
1	89	6	83	282.4
1.5	88	5	84	314.32
2	89	6	83	359.58
2.5	89	5	84	382.52
3	89	5	84	396.22

Table 18: Generated flux with respect to time (0.5 hr.)

Time (hr.)	Flux (lit/m^2hr.)
0.5	21.2778
1	15.1715
1.5	16.6096
2	17.8819
2.5	16.1130
3	14.2438

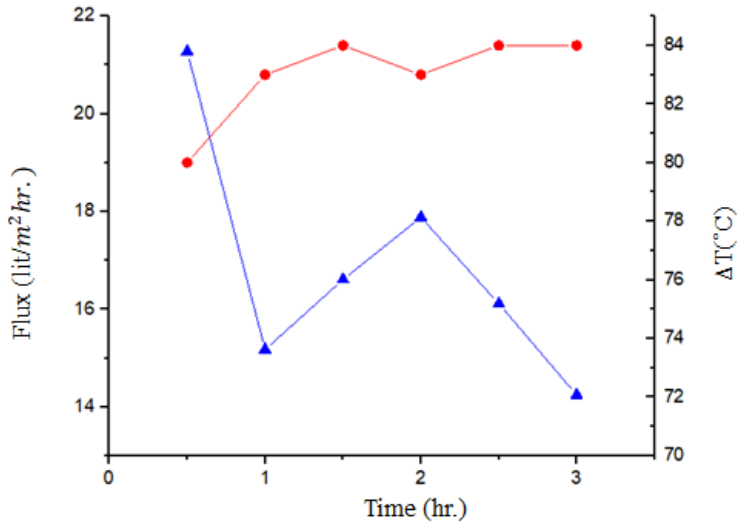

Temperature gradient (º C)
Flux (lit/m^2hr.)

Fig.26. Graphical representation of flux for 0.22µm PTFE with respect to time and temperature gradient (80 ºC to 86 ºC).Where Red color indicates the temperature gradient and blue color indicates the flux.

(a) (b)

Fig.27. Crystallization of salts after 4 hours (a) in feed tank(b) in reheating tank

➢ Observation

Salts were crystallized after 4 hours. Salts were absent in permeate (cold) side. Heat loss was compensate thereby desired temperature gradient was maintained. . Hence, Flux was improved in case of modified system as compare to unmodified Expt. #4.5.

- ***Phase 3: Optimization of temperature gradient (ΔT)***

.

4.7. Experiment with 0.22µm PTFE at ΔT 65ºC

Table 19: Temperature gradient and total dissolved solid (TDS) for hot side (70 ºC) and cold side temperature (5 ºC)

Time (hr.)	Hot side temp.(ºC)	Cold side temp.(ºC)	ΔT(˚C)	TDS(gm/lit)
0	71	5	66	145.18
0.5	73	6	67	165.1
1	71	6	65	189.62
1.5	70	6	64	193.02
2	70	7	63	196.44
2.5	70	6	64	203.8
3	69	6	63	262.82
3.5	72	5	67	256
4	72	6	66	272.14
4.5	72	6	66	261.98
5	72	6	66	254.72

Table 20: Generated flux with respect to time (0.5 hr.)

Time (hr.)	Flux (lit/m^2hr.)
0.5	26.8120
1	26.0403
1.5	18.3592
2	14.4969
2.5	12.7837
3	16.5780
3.5	13.7425
4	12.9590
4.5	11.0082
5	9.5564

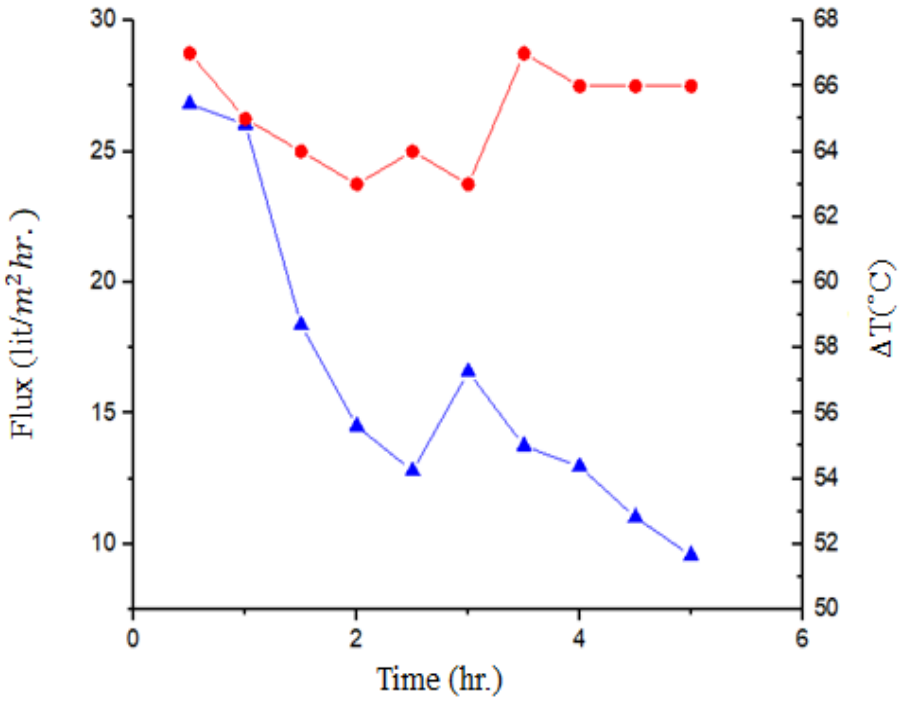

Temperature gradient (º C)
Flux (lit/m^2hr.)

Fig.28. Graphical representation of flux for 0.22 µm PTFE with respect to time and temperature gradient (63 ºC to 67 ºC).Where Red color indicates the temperature gradient and blue color indicates the flux.

➢ Observation

Flux was lower compared to expt. #4.6. Crystallization was occurred within 5 hours as compare to the expt. #4.6 which took 4 hours (ΔT was higher). Salts were not found in permeate side.

4.8.Experiment with 0.22µm PTFE at ΔT 65ºC

Table 21: Temperature gradient and total dissolved solid (TDS) for hot side temperature (85 ºC) and cold side temperature (20 ºC)

Time (hr.)	Hot side temp.(ºC)	Cold side temp.(ºC)	ΔT(˚C)	TDS(gm/lit)
0	85	18	67	175.34
0.5	81	20	61	186
1	83	22	61	196.58
1.5	82	22	60	222.52
2	83	21	62	247.86
2.5	84	21	63	296.8
3	85	21	64	334.48
3.5	85	21	64	323.9
4	85	21	64	336.2
4.5	83	22	61	407.46

Table 22: Generated flux with respect to time (0.5 hr.)

Time (hr.)	Flux(lit/$m^2hr.$)
0.5	12.7359
1	12.0052
1.5	15.7056
2	16.2546
2.5	18.18808
3	17.6216
3.5	14.5606
4	13.2907
4.5	14.0660

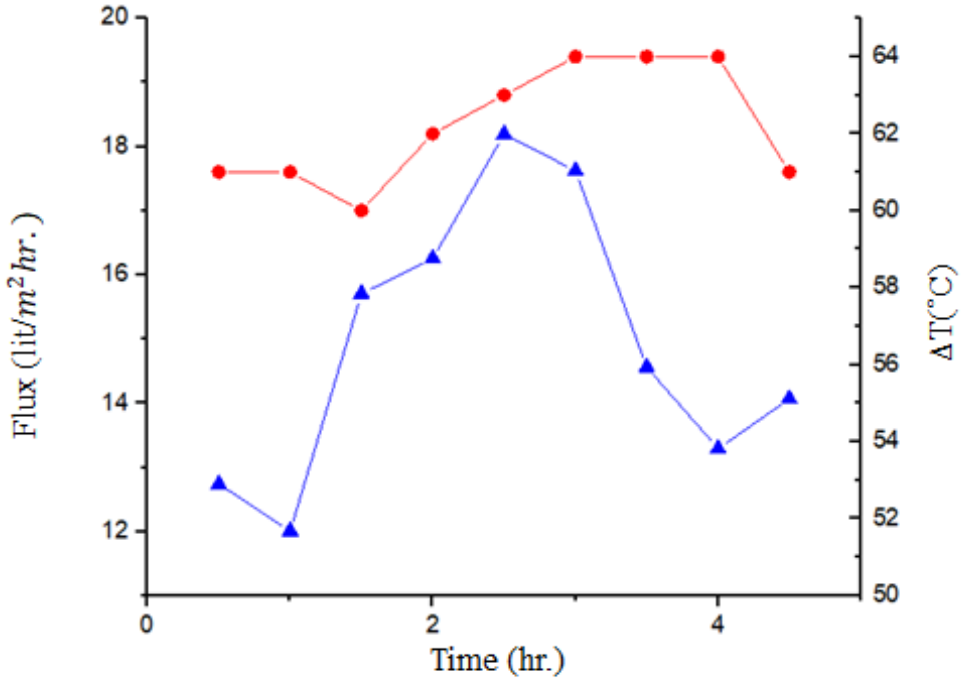

Temperature gradient (º C)
Flux (lit/m^2hr.)

Fig.29. Graphical representation of flux for 0.22 µm PTFE with respect to time and temperature gradient (60 ºC to 67 ºC).Where Red color indicates the temperature gradient and blue color indicates the flux.

➢ Observation

Flux has increased as compare to expt. #4.6 and expt. #4.7. Crystallization has occurred after 4.5hours.Salts were not present in permeate side.

- **Combined graph for 0.22µm PTFE membrane in three different ΔT range**

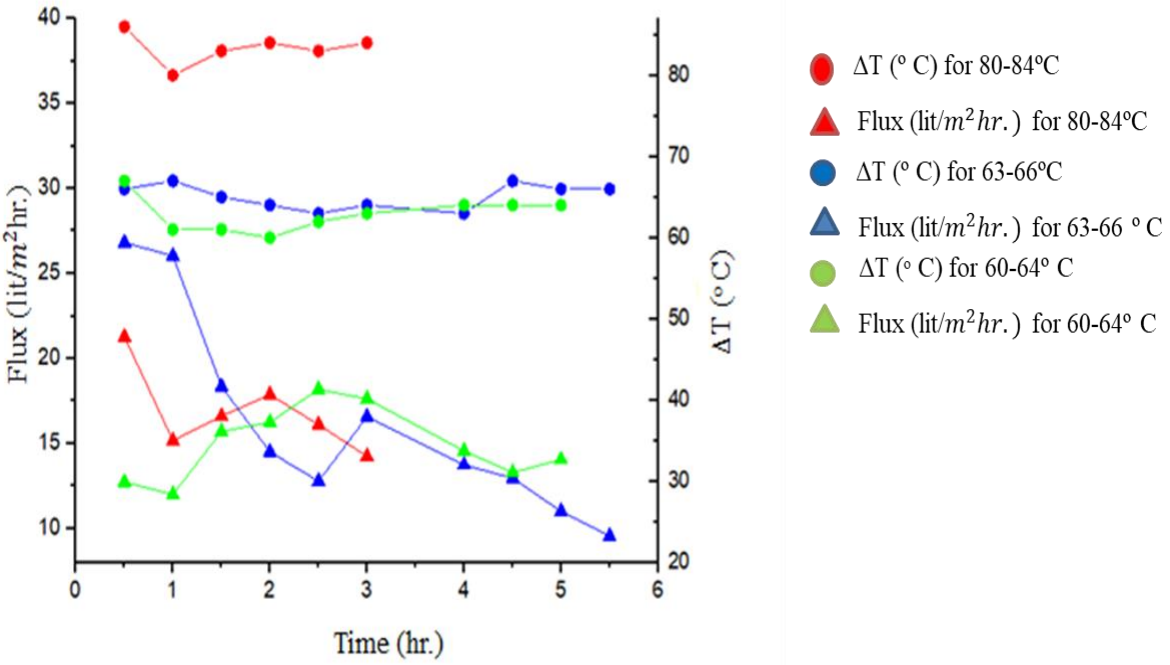

Fig.30. Graphical representation of fluxes with respect to time and varying temperature gradient of 0.22µm PTFE membrane .Where red color indicates the flux and temperature gradient at 80-84°C,blue color indicates the flux and temperature gradient at 63-66° C and green indicates the flux and temperature gradient at 60-64° C.

4.9.Experiment with 0.22 µm PVDF at ΔT 65º C

Table 23: Temperature gradient and total dissolved solid (TDS) for hot side temperature (85 ºC) and cold side temperature (20 ºC)

Time(hr.)	Hot side temp.(ºC)	Cold side temp.(ºC)	ΔT(ºC)	TDS (gm/lit)
0	81	18	63	223.82
0.5	86	20	66	230.98
1	84	21	63	289
1.5	85	21	64	328.96
2	85	21	64	367.04
2.5	85	20	65	398.14
3	86	21	65	402.58
3.5	86	21	65	425.66

Table 24: Generated flux with respect to time (0.5 hr.)

Time(hr.)	Flux(lit/$m^2hr.$)
0.5	6.88825
1	25.0595
1.5	23.6750
2	21.6779
2.5	19.4593
3	16.4457
3.5	15.0533

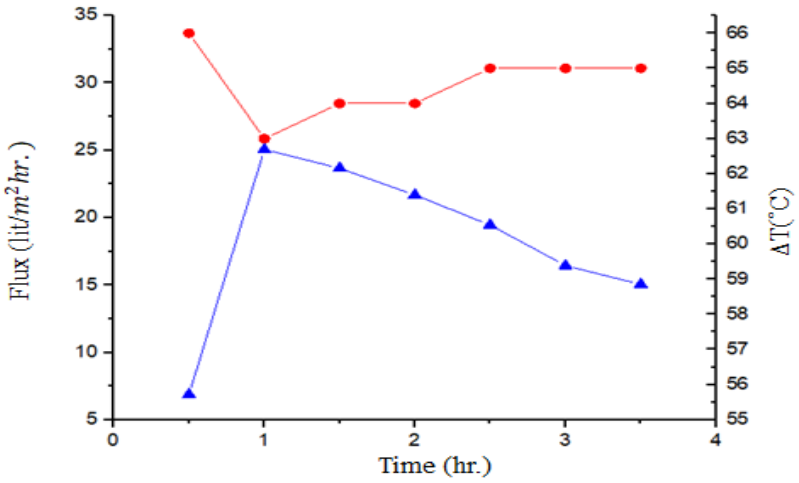

Fig.31. Graphical representation of flux for 0.22 µm PVDF with respect to time and temperature gradient (63 ºC to 66 ºC).Where Red color indicates the temperature gradient and blue color indicates the flux.

➢ Observation

Flux has increased significantly compare with PTFE (Expt. #4.6) and PP (Expt. #4.10).Crystallization has occurred within 3.25 hours. Salts were not found in the permeate side.

Fig.32. Crystallization of salts obtained in the process with 0.22 µm PVDF

4.10. Experiment with 0.22µm PP at ΔT 65 ºC

Table 25: Temperature gradient and total dissolved solid (TDS) for hot side temperature (85 ºC) and cold side temperature (20 ºC)

Time (hr.)	Hot side temp.(ºC)	Cold side temp.(ºC)	ΔT(ºC)	TDS(gm/lit)
0	85	18	67	212.72
0.5	85	20	65	224.42
1	85	21	64	261.46
1.5	84	20	64	260.56
2	84	20	64	256.78
2.5	86	21	65	306.18
3	83	20	63	334.74
3.5	83	20	63	351.02
4	82	20	62	345.38

Table 26: Generated flux with respect to time (0.5 hr.)

Time (hr.)	Flux(lit/$m^2hr.$)
0.5	11.58542
1	20.7127
1.5	13.6003
2	9.5325
2.5	13.5664
3	13.5008
3.5	12.5077
4	10.6694

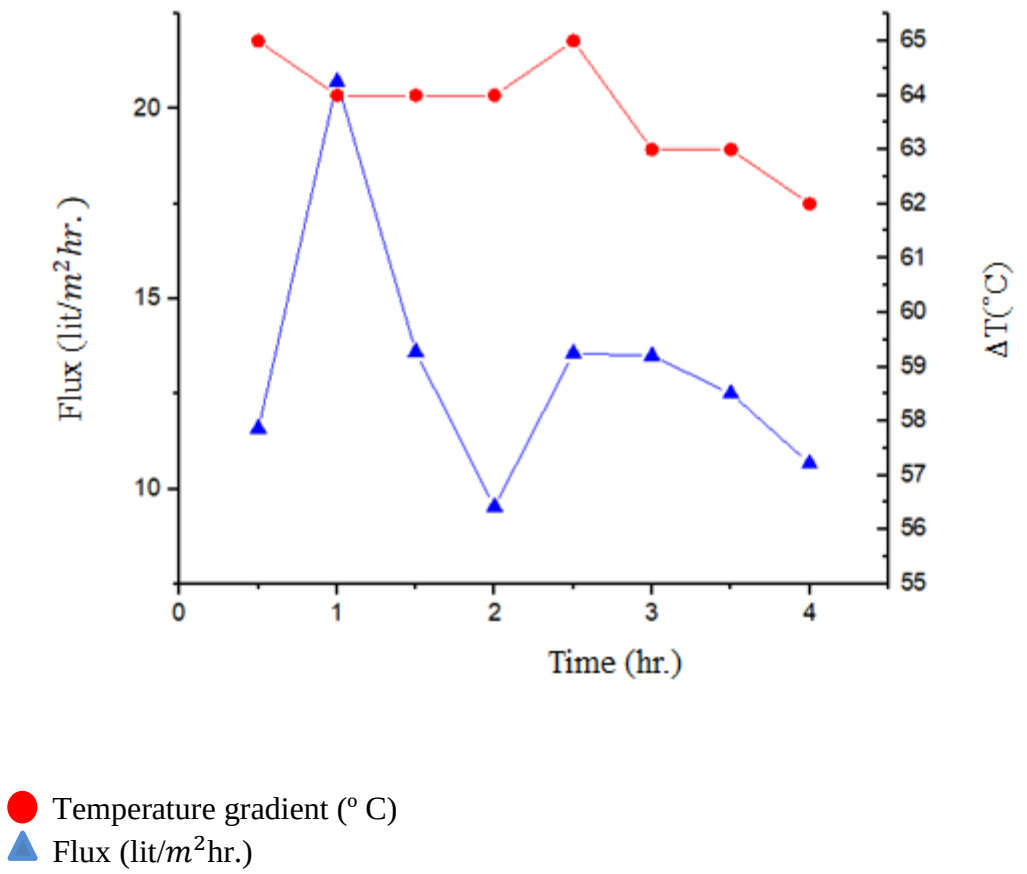

Fig.33. Graphical representation of flux for 0.22µm PP with respect to time and temperature gradient (62 ºC to 67 ºC).Where Red color indicates the temperature gradient and blue color indicates the flux.

➢ Observation

For PP membrane, flux has improved in modified system compared to the flux of unmodified DCMD set up (Expt.#1,2,3).in case of modified system.Previously flux was decreased rapidly but here flux has increased initially and finally decrease gradually.

Fig.34. Crystallization of salts for the process with PP membrane after 4 hours

➢ Combined graph for 0.22µm PVDF, PTFE and PP at 60to 65 ºC ΔT

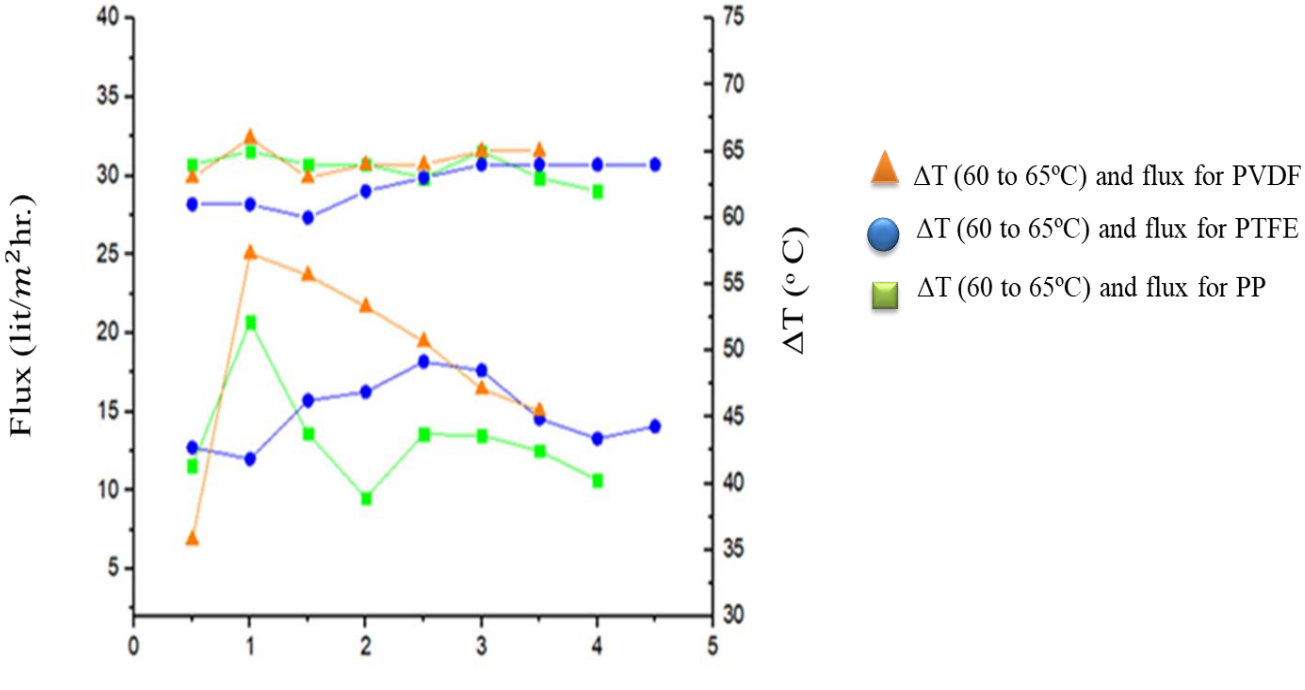

Fig.35. Graphical representation of fluxes with respect to time and varying temperature gradient of 0.22µm PVDF,PTFE and PP membrane. Where orange color indicates the flux and temperature gradient for 0.22µm PVDF, blue color indicates the flux and temperature gradient for 0.22µm PTFE and green indicates the flux and temperature gradient0.22µm PP at 60-65º C.

- ***Phase4:Flux determination for different membranes with the established ΔT range***

4.11. Experiment with 0.22 PVDF at ΔT 55ºC

Table 27: Temperature gradient and total dissolved solid (TDS) for hot side temperature (80 ºC) and cold side temperature (25 ºC)

Tim(hr.)	Hot side temp.(ºC)	Cold side temp.(ºC)	ΔT(ºC)	TDS(gm/lit)
0	80	24	56	196.66
0.5	82	25	57	201.36
1	77	25	52	221.4
1.5	78	25	53	232.9
2	79	25	54	236.02
2.5	79	25	54	241
3	80	25	55	217
3.5	80	25	55	248.14
4	80	25	55	264.76

Table 28: Generated flux with respect to time (0.5 hr.)

Time (hr.)	Flux (lit/$m^2hr.$)
0.5	5.1869
1	12.7471
1.5	11.5261
2	9.2647
2.5	8.1770
3	7.22
3.5	6.5861
4	7.0964

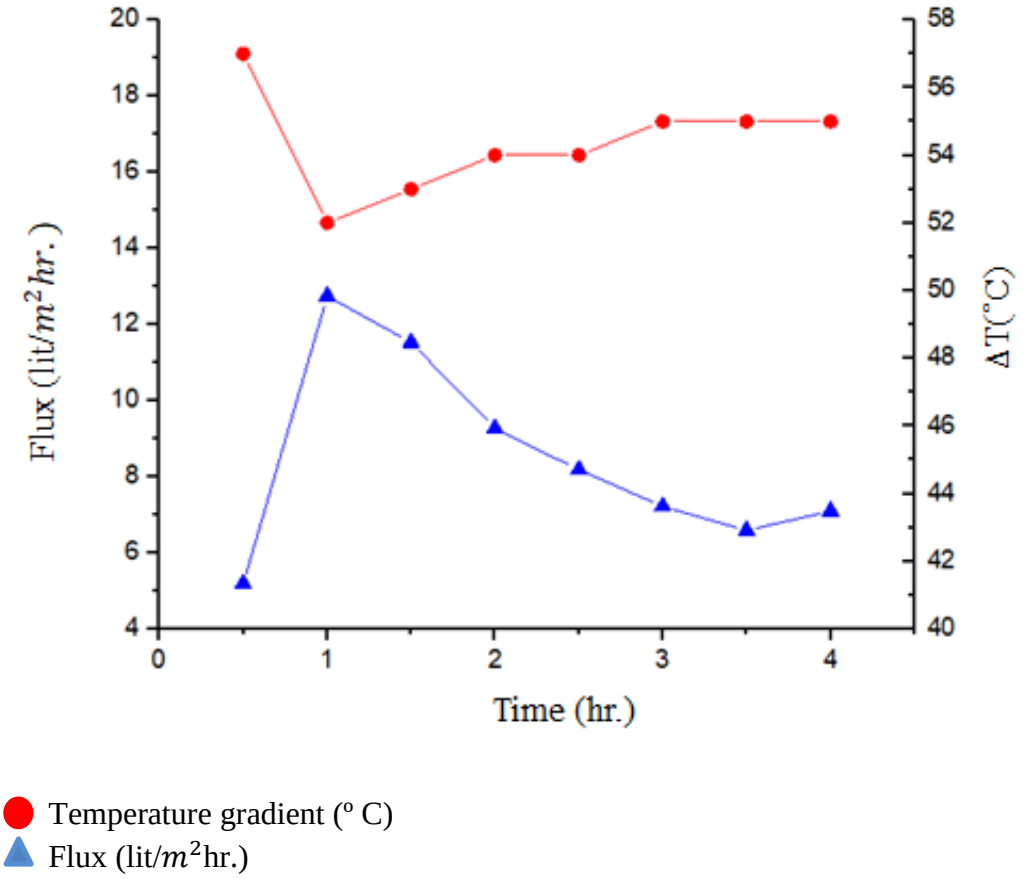

Fig.36. Graphical representation of flux for 0.22 µm PVDF with respect to time and temperature gradient (52 ºC to 57 ºC).Where Red color indicates the temperature gradient and blue color indicates the flux.

➢ Observation

The nature of the flux was same as Expt.4.9 but overall flut was decraesed as ΔT (55ºC) is lower than Expt.4.9 (65 ºC).Initially flus has increased and finally decreased gradually.

4.12. Experiment with 0.22 PVDF at ΔT 55ºC

Table 29: Temperature gradient and total dissolved solid (TDS) for hot side temperature (75 ºC) and cold side temperature (20 ºC)

Time (hr.)	Hot side temp.(ºC)	Cold side temp.(ºC)	ΔT(ºC)	TDS (gm/lit)
0	68	19	49	268.88
0.5	69	21	48	291.64
1	73	20	53	322.56
1.5	74	22	52	342.4
2	74	20	54	369.4
2.5	74	21	53	355.08
3	75	21	54	369.14
3.5	74	21	53	374.4
4	74	21	53	379.8
4.5	75	21	54	411.2
5	75	21	54	416.2

Table 30: Generated flux with respect to time (0.5 hr.)

Time (hr.)	Flux (lit/m^2hr.)
0.5	17.3425
1	18.4909
1.5	15.9051
2	15.1176
2.5	10.7894
3	10.055
3.5	8.9472
4	8.1124
4.5	8.7398
5	9.7089

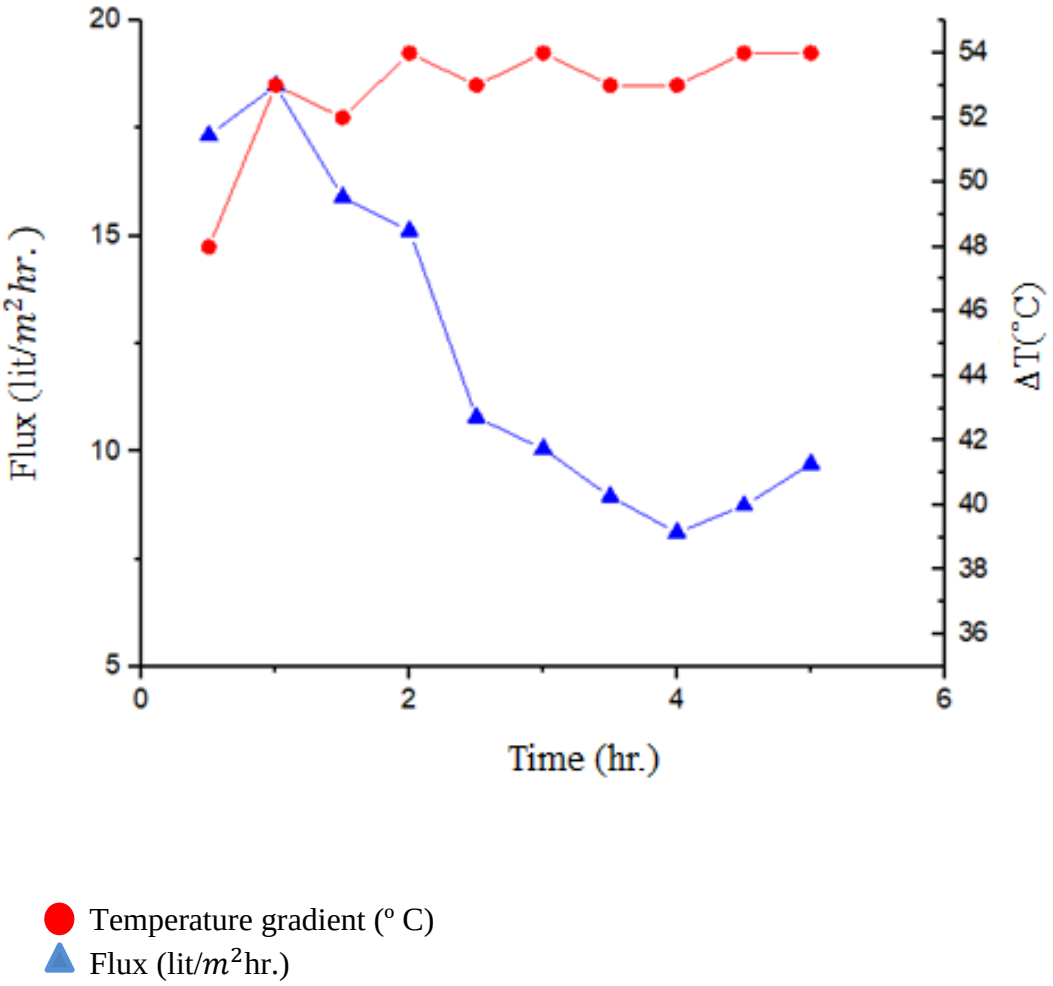

Fig.37. Graphical representation of flux for 0.22 µm PVDF with respect to time and temperature gradient (48 ºC to 54ºC).Where Red color indicates the temperature gradient and blue color indicates the flux.

➢ Observation

Flux was better than Expt.# 4.11 though the ΔT was same(55º C). PVDF showed better result when permeate and feed temp. was reduced by 5 ºC .In case of PTFE Expt. #4.6 showed better flux in higher ΔT range.

- **Combined graph for 0.22µm PVDF membrane in three different ΔT range**

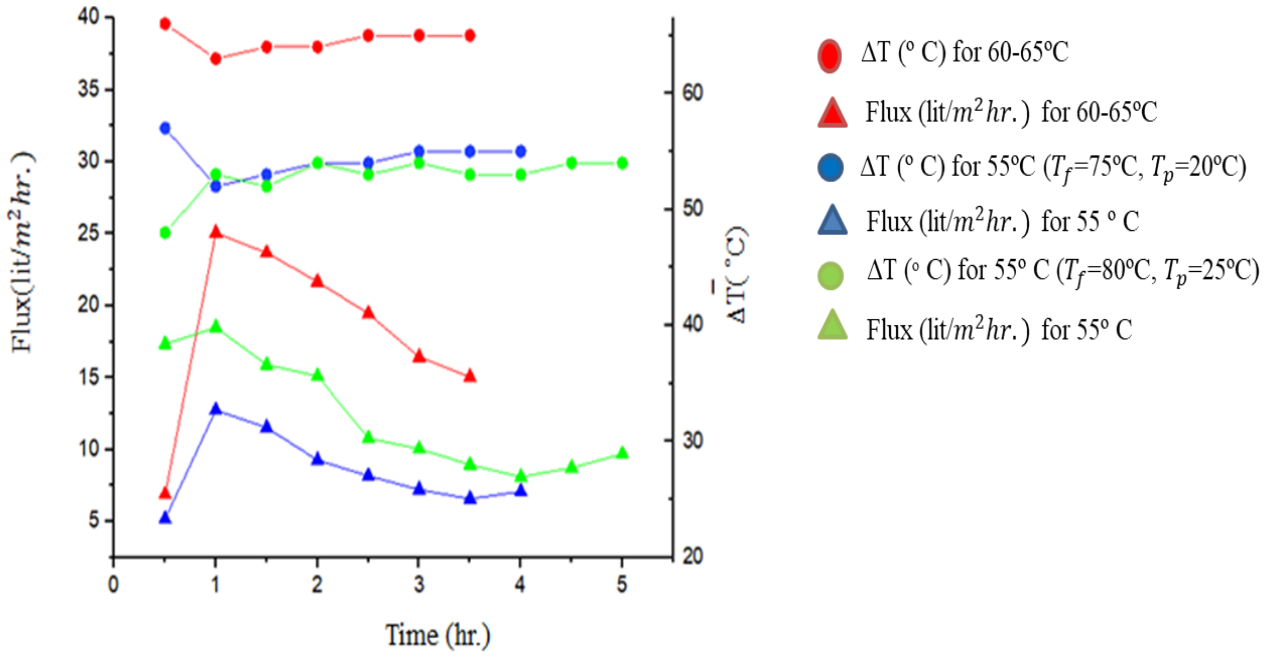

Fig.38.Graphical representation of fluxes with respect to time and varying temperature gradient of 0.22µm PTFE membrane .Where red color indicates the flux and temperature gradient at 60-65°C, blue color indicates the flux and temperature gradient at 55° C(T_f=75°C & T_p=20°C) and green indicates the flux and temperature gradient at 55° C(T_f=80°C & T_p=20°C).

- ***Phase4:Flux determination for different membranes with the established ΔT range***

4.13. Experiment with0.45µm PVDF at ΔT 65ºC

Table 31: Temperature gradient and total dissolved solid (TDS) for hot side temperature (85 ºC) and cold side temperature (20 ºC)

Time (hr.)	Hot side temp(ºC)	Cold side temp(ºC)	ΔT(ºC)	TDS(gm/lit)
0	85	18	67	212.72
0.5	83	20	63	236.48
1	84	21	63	251.04
1.5	83	21	62	279.04
2	81	21	60	241.36
2.5	85	21	64	263.44
3	83	20	63	264.44
3.5	82	21	61	291.42
4	81	21	60	347.46
4.5	82	20	62	341.72
5	83	21	62	339.16

Table 32: Generated flux with respect to time (0.5 hr.)

Time (hr.)	Flux (lit/m^2hr.)
0.5	22.3274
1	16.9605
1.5	17.6053
2	6.5922
2.5	8.5568
3	7.2438
3.5	8.5732
4	10.7718
4.5	9.3210
5	8.2845

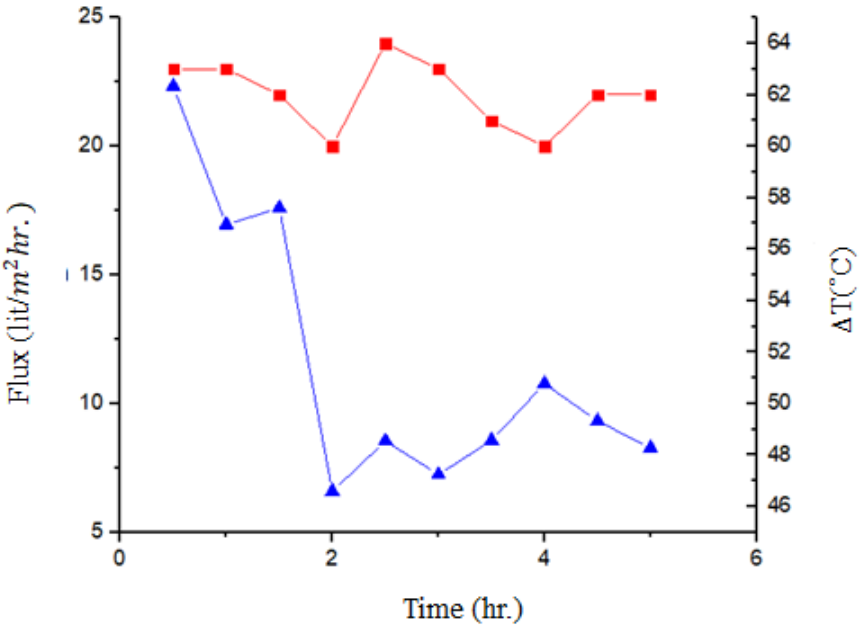

Temperature gradient (º C)
Flux (lit/m^2hr.)

Fig.39. Graphical representation of flux for 0.45 µm PVDF with respect to time and temperature gradient (60 ºC to 67 ºC).Where Red color indicates the temperature gradient and blue color indicates the flux.

➢ Observation

Both the average and the maximum fluxes were high.It took much time (5 hours) for complete crystallization than 0.22 µm (Expt.#4.9, 3.5 hours) when the ΔT was same 65 ºC.

4.14. Experiment with0.45µm PTFE at ΔT 65ºC

Table 33: Temperature gradient and total dissolved solid (TDS) for hot side temperature (85 ºC) and cold side temperature (20 ºC) with respect to time (0.5 hr.)

Time (hr.)	Hot side temp.(ºC)	Cold side temp.(ºC)	ΔT(ºC)	TDS(gm/lit)
0	85	20	65	226.76
0.5	83	21	62	236.24
1	82	21	61	243.92
1.5	84	21	63	301
2	82	22	60	299.18
2.5	82	21	61	315.26
3	84	21	63	379.8
3.5	84	20	64	360.98
4	84	20	64	377.3

Table 34: Generated flux with respect to time (0.5 hr.)

Time (hr.)	Flux (lit/m^2hr.)
0.5	8.9174
1	7.8167
1.5	18.2699
2	13.4478
2.5	12.4764
3	14.9240
3.5	11.8038
4	11.0831

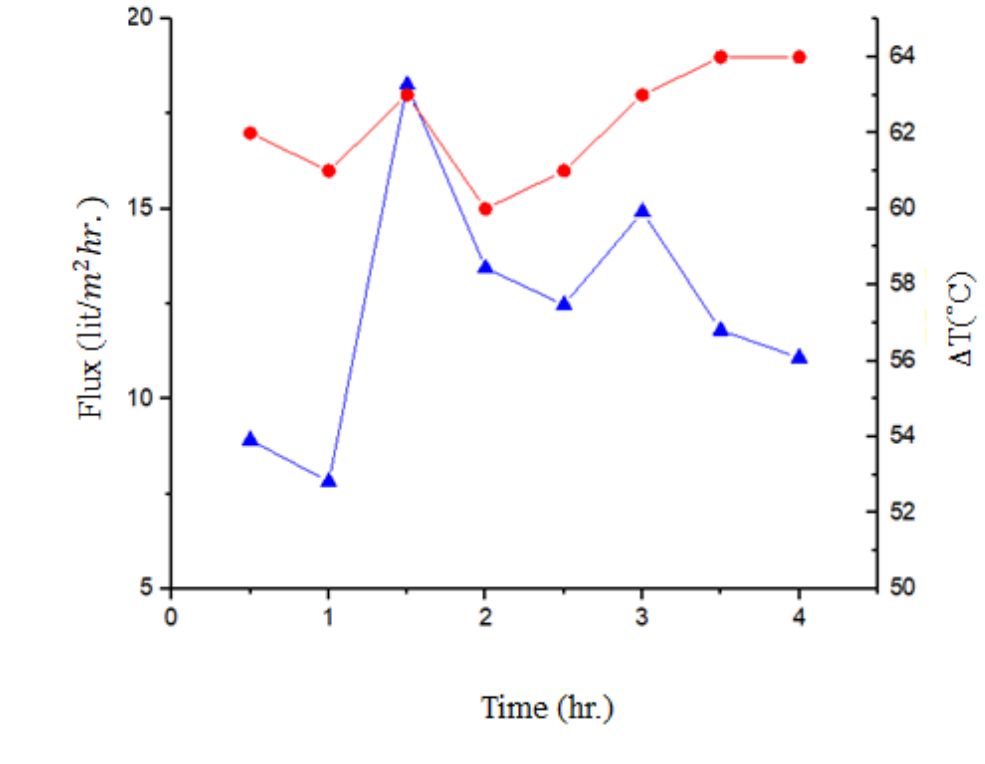

Fig.40: Graphical representation of flux for 0.45 µm PTFE with respect to time and temperature gradient (60 ºC to 65 ºC).Where Red color indicates the temperature gradient and blue color indicates the flux.

➢ Observation

Flux was lower than 0.45 µm PP (Expt.# 4.15) and PVDF (Expt. #4.13).0.22 µm PTFE (Expt.4.8) showed higher flux compare to 0.45 µm. Crystallization has occurred (4 hours)

4.15. Experiment with 0.45µm PP at ΔT 65ºC

Table 35: Temperature gradient and total dissolved solid (TDS) for hot side temperature (85 ºC) and cold side temperature (20 ºC)

Time (hr.)	Hot side temp.(ºC)	Cold side temp.(ºC)	ΔT(ºC)	TDS(gm/lit)
0	85	20	65	208.1
0.5	84	20	64	228.2
1	84	21	63	231.62
1.5	83	20	63	259
2	82	20	62	247.52
2.5	85	21	64	280.84
3	84	21	63	300.02
3.5	85	20	65	335.5
4	85	20	65	357.92
4.5	85	20	65	382.84

Table 36: Generated flux with respect to time (0.5 hr.)

Time (hr.)	Flux (lit/m^2hr.)
0.5	19.5024
1	11.2828
1.5	14.5574
2	8.8477
2.5	11.5114
3	11.3473
3.5	12.0549
4	11.6273
4.5	11.2698

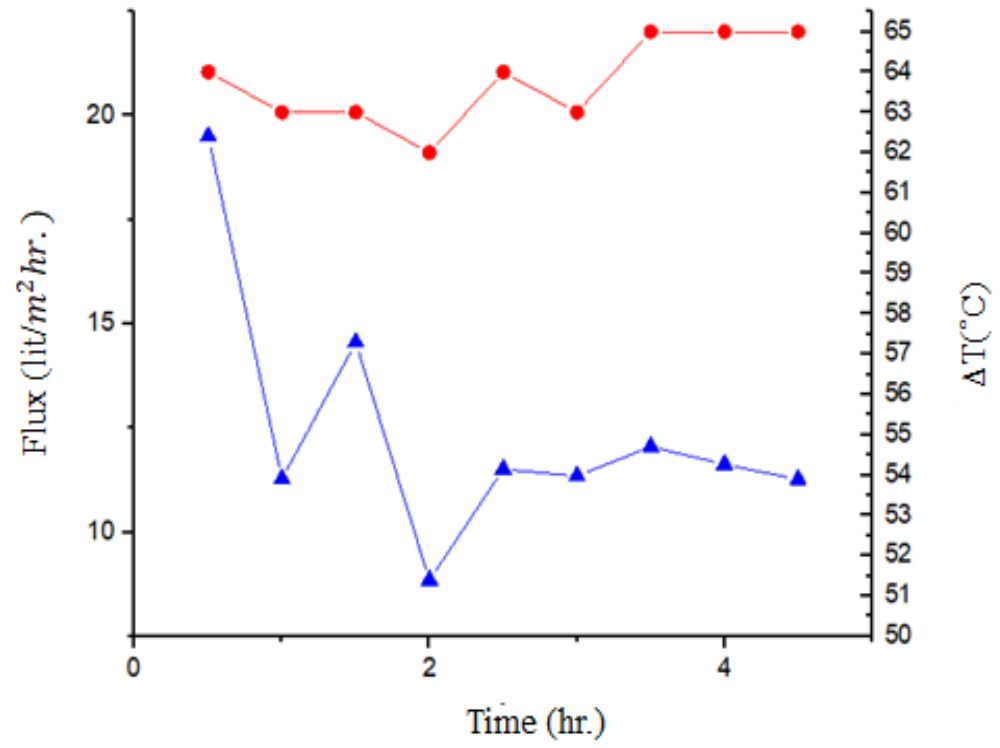

Fig.41. Graphical representation of flux for 0.45 µm PP with respect to time and temperature gradient (62 ºC to 65 ºC).Where Red color indicates the temperature gradient and blue color indicates the flux.

➢ Observation

The average flux value was resanoble .The maximum flux was similar to 0.22 µm PP (Expt. #4.10). Crystallization has occurred with in 4.5 hours.

- **Combined graph for 0.45µm PVDF, PTFE and PP at 60to 65ºC ΔT**

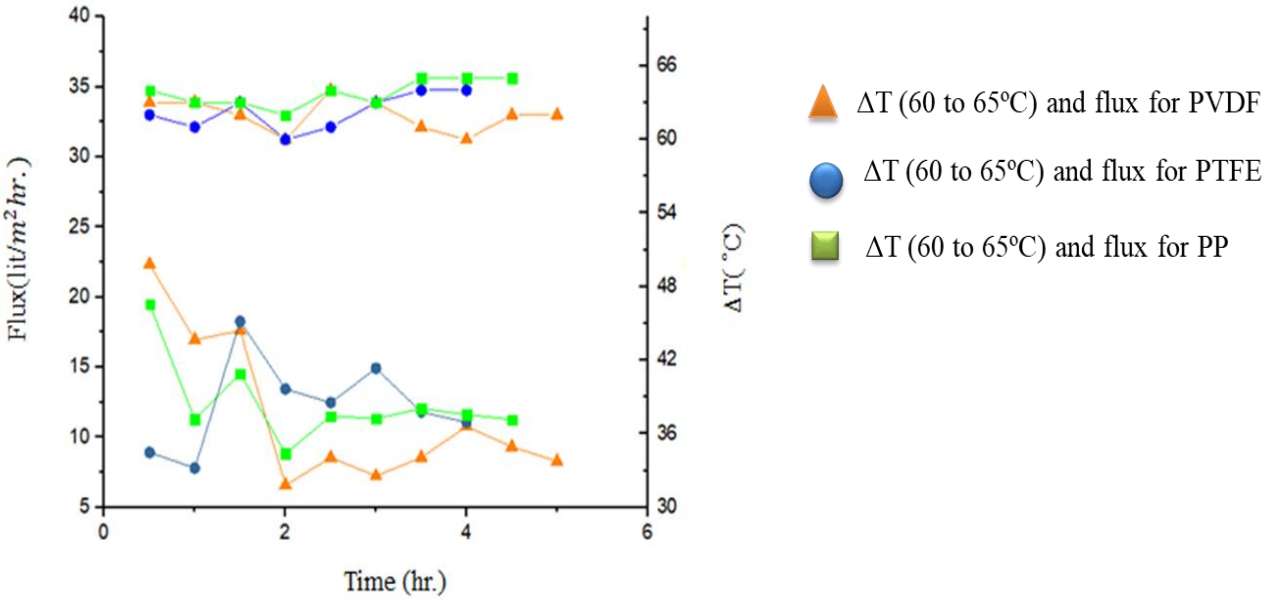

Fig.42. Graphical representation of fluxes with respect to time and temperature gradient of 0.22µm PVDF,PTFE and PP membrane .Where orange color indicates the flux and temperature gradient for 0.22µm PVDF, blue color indicates the flux and temperature gradient for 0.22µm PTFE and green indicates the flux and temperature gradient0.22µm PP at 60-65º C.

4.16. Experiment with1µm PVDF at ΔT 65ºC

Table 37: Temperature gradient and total dissolved solid (TDS) for hot side temperature (85 ºC) and cold side temperature (20 ºC)

Time (hr.)	Hot side temp.(ºC)	Cold side temp.(ºC)	ΔT(ºC)	TDS(gm/lit)
0	85	20	65	225.38
0.5	79	22	57	229.6
1	79	21	58	249.26
1.5	77	21	56	251.46
2	77	20	57	268.14
2.5	79	22	57	290.32
3	80	22	58	292.66
3.5	79	20	57	297.12
4	83	23	60	316.68
4.5	84	22	62	332.8

Table 38: Generated flux with respect to time (0.5 hr.)

Time (hr.)	Flux (lit/m^2hr.)
0.5	4.0843
1	11.9754
1.5	7.6825
2	8.8593
2.5	9.9415
3	8.5144
3.5	7.6651
4	8.0084
4.5	7.9697

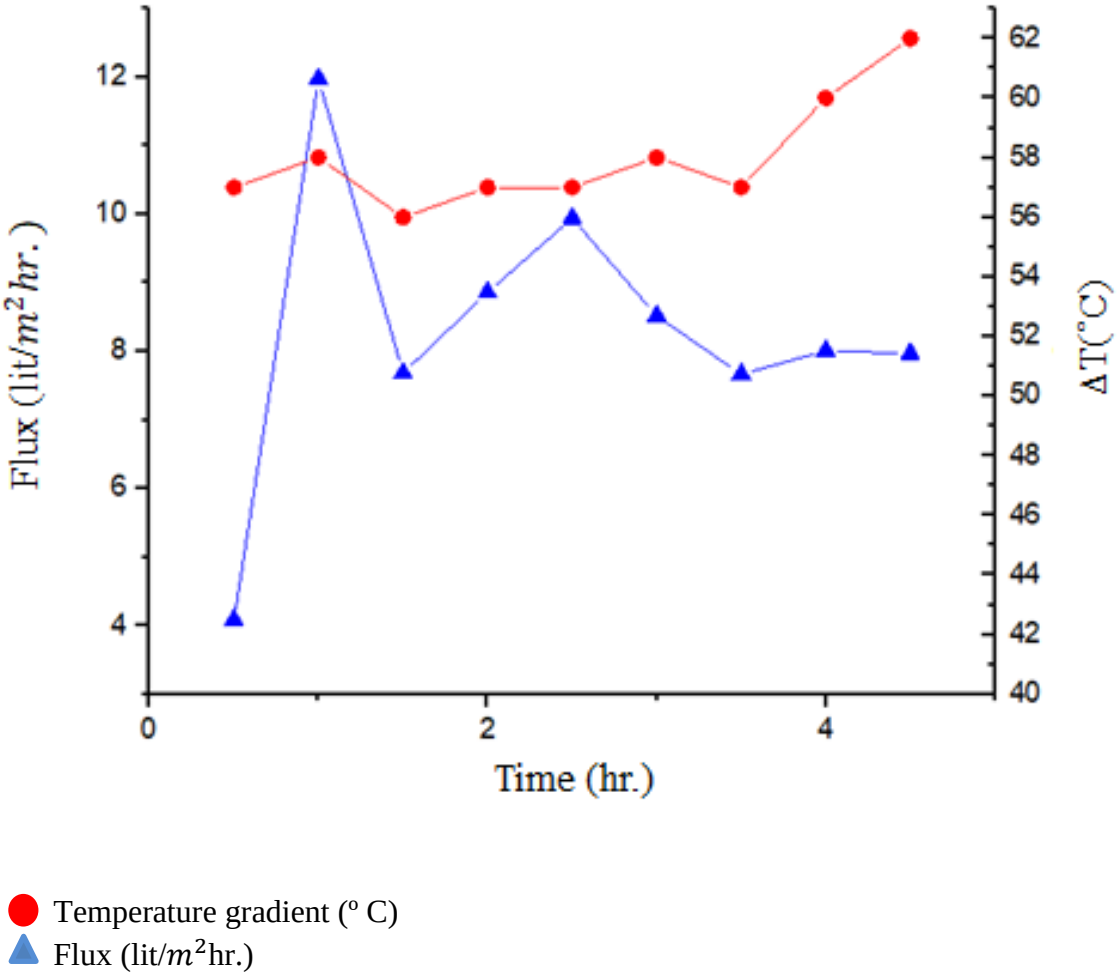

Fig.43. Graphical representation of flux for 1 µm PVDF with respect to time and temperature gradient (56 ºC to 65ºC).Where Red color indicates the temperature gradient and blue color indicates the flux.

➢ Observation

As the flux was lower, time for crystallization (4.5 hours) was high.Average flux was lower than 0.45µm and 0.22 µm PVDF (Expt.#4.13,#4.9) membrane at same ΔT 65 ºC.

4.17. Experiment with 1 µm PTFE at ΔT 65ºC

Table 39: Temperature gradient and total dissolved solid (TDS) for hot side temperature (85 ºC) and cold side temperature (20 ºC)

Time (hr.)	Hot side temp.(ºC)	Cold side temp.(ºC)	ΔT(ºC)	TDS (gm/lit)
0	85	20	65	200.1
0.5	84	21	63	239.52
1	84	21	63	275.58
1.5	85	20	65	255.24
2	85	21	64	265.36
2.5	82	20	62	278.06
3	84	21	63	286.58
3.5	85	21	64	293.3
4	85	21	64	311.2
4.5	85	20	65	283.66

Table 40: Generated flux with respect to time (0.5 hr.)

Time (hr.)	Flux (lit/m^2hr.)
0.5	36.5731
1	30.4327
1.5	16.0023
2	13.6058
2.5	12.4609
3	11.1765
3.5	9.5798
4	9.9168
4.5	7.2735

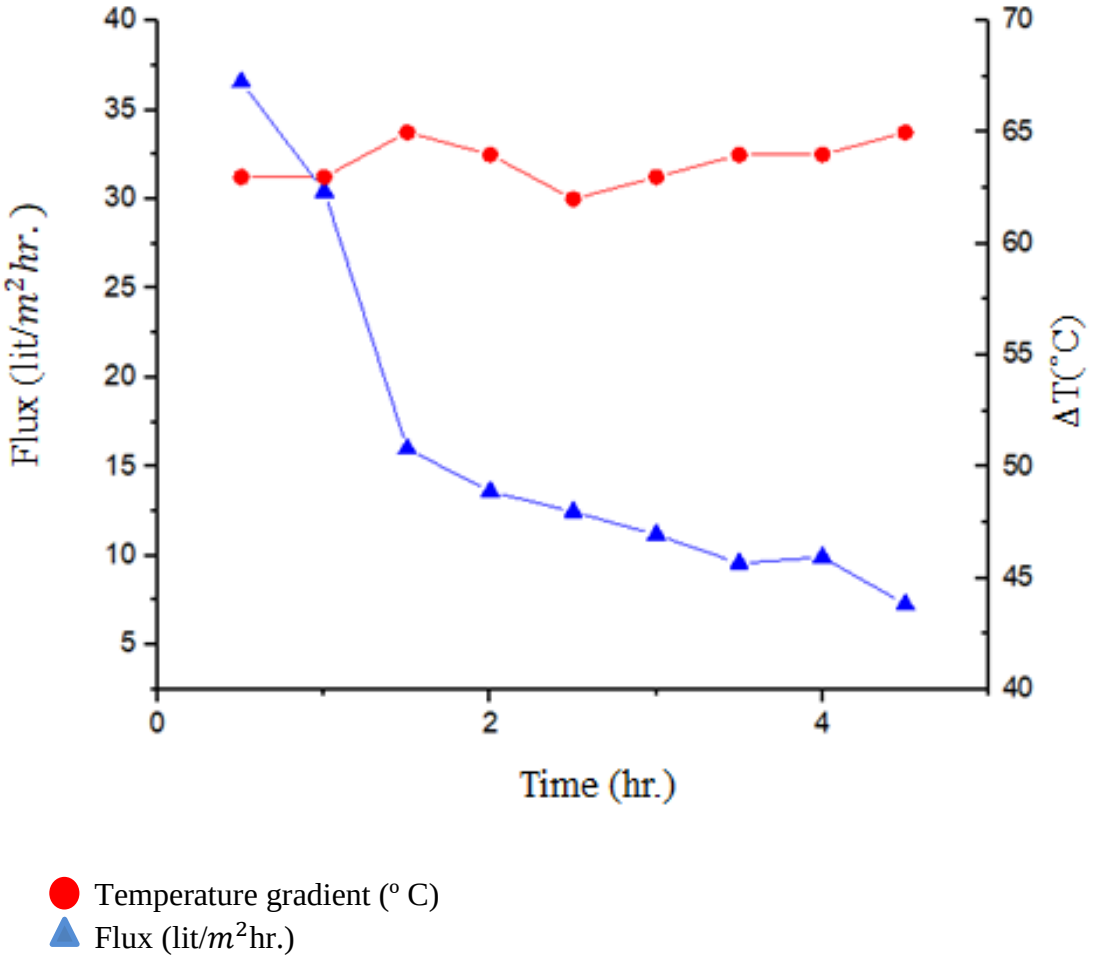

Fig.44. Graphical representation of flux for 1 µm PTFE with respect to time and temperature gradient (62 ºC to 65 ºC).Where Red color indicates the temperature gradient and blue color indicates the flux.

➢ Observation

Initial flux was very high with higher ΔT value but gradually decreased over time. Time for crystallization (3 hours) was less than PP and PVDF

4.18. Experiment with 1µm PP at ΔT 65 ºC

Table 41: Temperature gradient and total dissolved solid (TDS) for hot side temperature (85 ºC) and cold side temperature (20 ºC)

Time (hr.)	Hot side temp.(ºC)	Cold side temp.(ºC)	ΔT(ºC)	TDS (gm/lit)
0	85	20	65	220.44
0.5	85	22	63	225.06
1	82	21	61	231.32
1.5	79	20	59	261.94
2	80	20	60	243.98
2.5	78	23	55	296.1
3	78	21	57	269.24
3.5	78	22	56	289.74
4	78	22	54	256.09

Table 42: Generated flux with respect to time (0.5 hr.)

Time (hr.)	Flux (lit/m^2hr.)
0.5	4.5617
1	5.226
1.5	11.7357
2	5.3601
2.5	11.3565
3	6.7129
3.5	7.593
4	3.8669

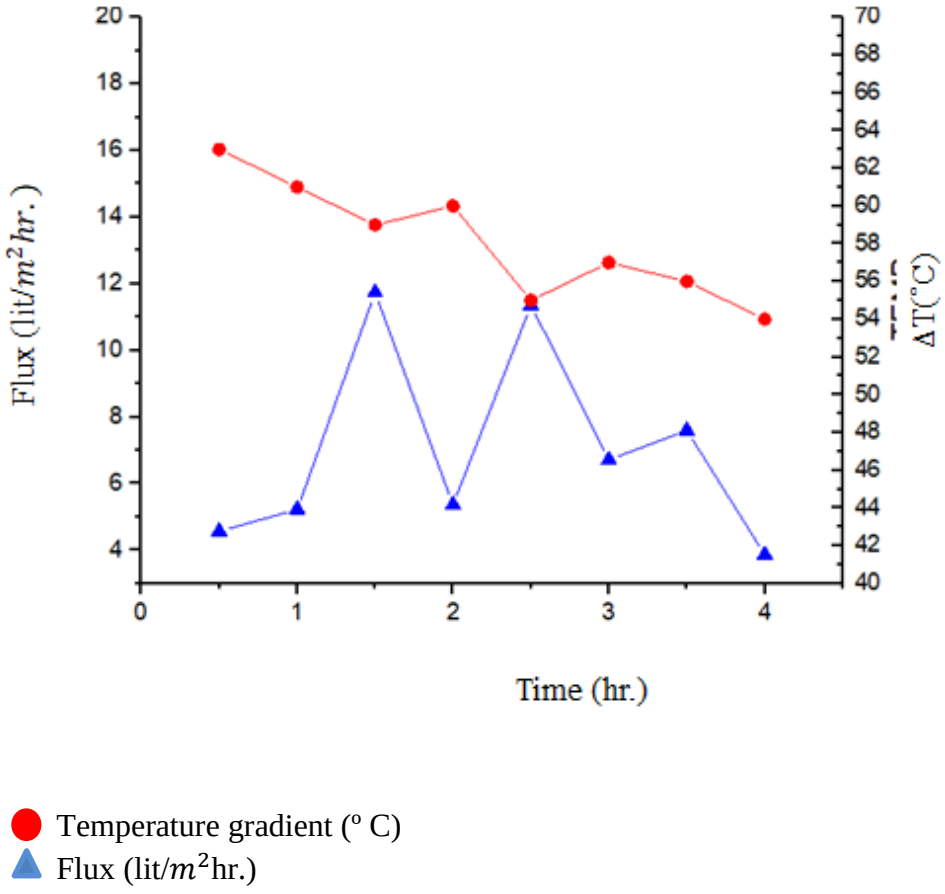

Fig.45. Graphical representation of flux for 1 µm PP with respect to time and temperature gradient (54 ºC to 65 ºC).Where Red color indicates the temperature gradient and blue color indicates the flux.

➢ Observation

Flux has increased initially and then decreased with the increase in TDS. Fluxes were approximately same as PVDF (Expt. #4.16) but lower than PTFE (Expt. # 4.18).Crystallization has (after 4 hours).Heat loss was higher than PTFE (Expt. # 4.17) and PVDF

➢ Combined graph for 1µm PVDF, PTFE and PP at 60to 65ºC ΔT

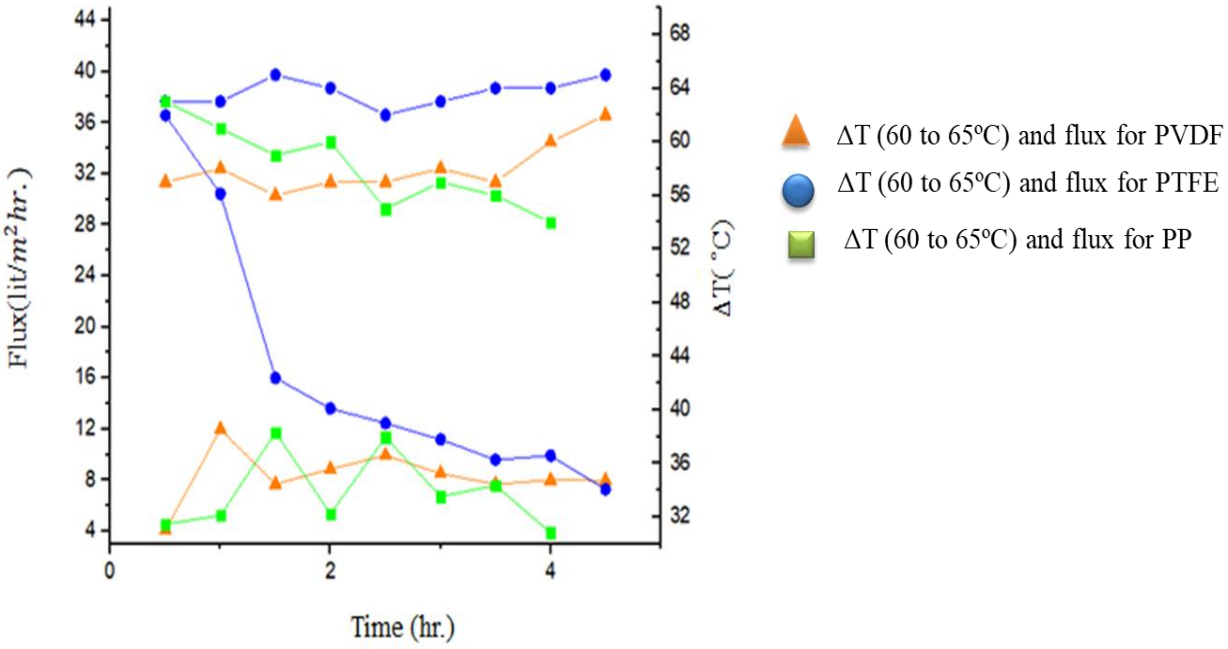

Fig.46. Graphical representation of fluxes with respect to time and temperature gradient of 0.22µm PVDF, PTFE and PP membrane .Where orange color indicates the flux and temperature gradient for 0.22µm PVDF, blue color indicates the flux and temperature gradient for 0.22µm PTFE and green indicates the flux and temperature gradient0.22µm PP at 60-65º C.

- Calculation

Flux was calculated by the following formula

$$\text{Flux} = \frac{\text{volume transfered from hot side to permeate side(lit)}}{\text{mass transfer area}(m^2)*\text{time(hr.)}}$$

The volume of water which transferred as vapor from hot side to permeate side was calculated by $V_1*S_1=V_2*S_2$

Where, V_1 & V_2 are TDS of feed samples at 30 minutes interval. Mass transfer area is $0.045m^2$.

Table 43: Summary of the results of PP and PTFE membrane without reheating

Membrane Type	Expt. no #	Pore dia. (µm)	Hot temp. (ºC)	Cold temp.(ºC)	ΔT(highest actually attained) (ºC)	Reheating	Maxm. TDS (gm/lit)	Maxm. Flux (lit/m^2 hr.)	Avg. Flux (lit/m^2hr.)	Time require for crystallization (hr.)	Salts transferred to permeate
PP	1	0.45	70	5	62	No	209.44	5.9	4	No crystallization	Yes
	2	0.22	75	5	66	No	287.22	13.9	5.3	No crystallization	Yes
	3	0.22	90	15	76	No	262.76	20.3	6.92	No crystallization	No
PTFE	4	0.22	70	5	61	No	239.8	11.6	3.4	No crystallization	No
	5	0.22	90	5	83	No	263.4	16.9	10.1	No crystallization	No

Table 44: Summary of the results of PP, PTFE and PVDF with reheating

Membrane Type	Expt. no #	Pore dia. (µm)	Hot temp. (ºC)	Cold temp.(º C)	ΔT(highest actually attained) (ºC)	Reheating	Maxm. TDS (gm/L)	Maxm. Flux (lit/ m^2hr.)	Avg. Flux (lit/ m^2hr.)	Time require for crystallization (hr.)	Salts transferred to permeate
PTFE	6	1	85	20	65	Yes	311.2	36.6	16.3	4.75	No
	7	0.45	85	20	65	Yes	377.3	18.3	12.34	4	No
	8	**0.22**	**90**	**5**	**86**	**Yes**	**396.2**	**21.3**	**16.9**	**3**	**No**
	9	0.22	70	5	67	Yes	272.1	26.8	16.2	4.75	No
	10	0.22	85	20	67	Yes	407.5	18.2	15	4.5	No
PVDF	11	1	85	20	65	Yes	332.8	12	8.3	4.5	No
	12	0.45	85	20	67	Yes	347.46	22.3	11.6	5	No
	13	**0.22**	**85**	**20**	**66**	**Yes**	**425.7**	**25.1**	**18.3**	**3.25**	**No**
	14	0.22	80	25	57	Yes	264.7	12.7	8.5	4.0	No
	15	0.22	75	20	54	Yes	416.2	18.5	12.32	5.0	No
PP	16	1	85	20	65	yes	289.7	11.7	7.05	4	No
	17	0.45	85	20	65	yes	382.8	19.5	12.44	4	No
	18	0.22	85	20	65	yes	351	20.7	13.2	4.25	No

Chapter 5
Discussion

Chapter 5

Discussion

The aim of this project is to desalinate the spent media after the production of bioplastic polymers by *Haloferax mediterranei.* Therefore, a feasibility study was conducted to investigate the desalination by direct contact membrane distillation process (DCMD). As our main focus was the desalination not the PHA production, we desalinated the growth media (MST) maintaining the salt concentration required for growth of *Haloferax sp.* However, the initial and final salt concentration of the process was same. The salt concentration for PHA production was approximately 225.5 gm/lit. Though this high salt concentration allows the process without sterilization, but its disposal is the huge problem as this high TDS effluent can't be discharged as per environmental norms. So, a post treatment process was mandatory in order to lower the TDS value. Application of DCMD for desalination of bioplastic spent media is very new to this field; previously a two stage desalination process was done by Bhattacharyya et al. This method, first demonstrated in a laboratory beaker was subsequently scaled up in a cylindrical baffled-tank with an immersed heater and a stirrer holding axial and radial impellers (Bhattacharyya et al. 2015). Although this process exhibited 99.3% salt rejection but it may not be suitable for commercialized scale-up processes. The cost of decanoic acid and the difficulties of its recycling increases the overall cost for desalination. The application of DCMD for high TDS has not been investigated before. This study is supported by that of Rao and Li (2015) where the author reported that DCMD was capable of treating flowback/produced water with high TDS value of 280 g/lit and fluxes were always greater than 15 L/m^2h. Stable water fluxes were observed over the 5-h test at all the investigated temperatures for all the membranes tested and more than 99.8% salt rejection was achieved in each test. Flux values similar to that of Rao and Li (2015) as well as salt separation were also obtained in our study.

Earlier experiments were performed in simplest DCMD configuration in order to acquire baseline data. These data were further compared with the modified configurations with reheating system. This study evaluated the effects of feed temperature, temperature difference across the membrane (ΔT), and permeate flux generation.

- Effect of feed temperature gradient on flux

Table 43 and 44 represents the overall performance data of the three membranes (PP, PTFE and PVDF) at different temperature gradients across the membrane. In DCMD, the driving force for mass transfer is the vapor pressure difference that develops from the temperature difference between the liquid phases on both sides of the membrane (Zhang et al. 2010) We have observed that the fluxes exhibited an exponential dependence on temperature—as would be expected when considering the Antoine equation for vapor pressure of water:

P^v= exp (23.328-($\frac{3841}{T-45}$))

Where *p* is the vapor pressure of water in Pa and *T* is the temperature in K.

We observed that there was rapid decline of ΔT in the earlier experiments due to the conductive heat loss from hot side to cold side. This rapid decline in ΔT resulted poor flux generation. So, in the next set of experiments a reheating system was introduced in the hot side exit which will compensate the heat loss. It was also observed that without reheating (see Table no.43, 44) crystallization occurred. However, reheating system maintained the set ΔT values throughout the process and increased the process efficiency by crystallization of salts.

The maximum and average flux values were high when the ΔT value was highest (Expt. #8, Table 44), it also took less time for crystallization .We observed that the hot and cold side temperature played an important role for mass flux generation, so higher feed temperature resulted better fluxes. In case of Expt. # 14 and 15, it was observed that increase in feed temperature by 5°C decreased the crystallization time by an hour. Zhang et al. (2010) studied the DCMD performances with various membrane in different temperature and inlet velocities and observed that increased in inlet temperature also increasing the permeate flux. As MD is thermally driven process driven by vapor pressure differences which vary exponentially with the feed temperature. Moreover, in the second phase of this investigation different ΔT ranges were investigated for PTFE membrane, it showed reasonable flux at ΔT 65ºC when feed and permeate temperatures were 85 ºC and 20 ºC, respectively. Therefore, temperature gradient has been identified as an important operating condition for DCMD process. Higher operating temperatures were preferable for improvement in heat and mass transfer.

- Effect of evaporation

Since the whole set up was not a thermodynamically close system, evaporation occurred from hot feed surface when the feed temperature was high. However, this evaporation process also enhanced the process by mass transfer to the atmosphere. Although some portion of heat loss occurred, this was compensated by reheating the cool brine reject and returned back to the primary reservoir. An experiment has been conducted in this investigation to check such evaporative loss at 85ºC. 250 ml solution was evaporated within 5 hours.

- Effect of feed concentration

Another important observation in this investigation was that water flux decreased with increasing feed water concentration (TDS), likely due to the reduction of the vapor pressure difference (Rao and Li 2015). The flux declined over time and though it was more significant at high concentration. This was due to the effect of concentration and temperature polarization. When the feed solution became viscous and concentrated, it reached its saturation point and crystallization occurred. The salt crystals deposited on the membrane

surface and subsequently blocked the pores of the membrane. As a result this clogging of pores reduced the permeability of the membrane and thus restricted mass transfer process. This caused rapid reduction is flux generation. Also, there was a 20% reduction of salt crystal formation and an 8% decline of transmembrane flux for natural reverse osmosis brines due to the existence of dissolved organic matter, which may be comparable with this study because yeast extract was present in the feed (Ashoor et al. 2016; Camacho et al. 2013)

- Effect of membrane properties

The properties of membrane have a great influence on heat and mass transfer in DCMD. This study was performed with three different polymeric flat sheet membranes (PP, PTFE, PVDF) which have different thickness, contact angle, surface energy. These differences in membrane properties also change the generated flux under different operating conditions. The experiments were performed with three pore sizes (1µm, 0.45µm and 0.22µm) for each membrane. It was found that higher pore size did not have much influence in flux. In some experiments, better fluxes were obtained for 0.22µm than 0.45µm and 1µm. However, previous investigations showed that increasing pore size might increase the flux for different MD processes. Although mass flux has no dependency on pore size for molecular diffusion, whereas
Knudsen diffusion increases with increase in pore diameter.

The flux values are similar for Expt. # 8 and #13, though the ΔT value was lower by 20 ° C for Expt. # 8 than Expt. #13. This result implicates that different membrane properties may influences the flux. The thickness of PVDF membrane is lower than PP and PTFE and more hydrophobic in nature. This lower thickness showed better flux though the conductive heat loss greater for PVDF than PP and PTFE. The thickness should be in an optimum range, so that it can withstand the heat loss as well as maintain a better flux (Eykens et al. 2016). We observed best results for Expt. # 8 and #13. Comparing these two flux values, PVDF showed better result that PTFE and PP. High contact angle, high surface energy and low thermal conductivity of PVDF makes it more hydrophobic which maintains the LEP and prevents pore wetting. Also the lower thermal conductivity of PVDF makes it more preferable for the desalination purpose.

- Effect of Liquid entry pressure (LEP) on flux

Liquid entry pressure or LEP should be higher than the hydrophobic pressure of feed water in between the DCMD module. Lower LEP causes transfer of water molecule instead of vapor molecules. This pore wetting was arrested in our earlier experiments performed in simplest DCMD configuration. In Expt. #1 and #2 we found salts in the permeate side which indicated lower LEP than the hydrophobic pressure. As a result the feed temperature declined very rapidly thus poor flux was obtained.

- Economic benefits

It is very difficult to evaluate cost analysis of full-scale performance based on bench scale performance results. In this study, Pilot scale tests were performed in ordered to desalinate high TDS spent effluent. One of the most important advantages of the DCMD process for desalination is, it shows the relatively minimal effect of feed salt concentration on the performance of the system than RO. In DCMD, it has been seen that increased feed salt concentration only decreases the flux when the feed become viscous and reached its saturation point. But in RO, increased feed salt concentration significantly decreases the driving force for mass transport and also increases transfer of salt through the membrane. DCMD can be operated below the boiling point of water, this makes this process economic than RO. As it requires low operating temperature, renewable solar or geothermal energy could be utilized to heat the feed water. DCMD requires two pumps for the feed and permeate. Maximum pressure for feed side was observed 5 to 10 psi which was relatively lower as compared to RO operation. Low pressure pumps are preferable for both capital and operating costs.

Chapter 6
Conclusion

➢ Conclusion

This study was a new approach for the design and operation of DCMD for desalination of growth medium of *Haloferax mediterranei*, a producer of polyhydroxyalkanoate bioplastic. Here, it was demonstrated that careful design of a membrane module and configuration of MD system could reduce the LEP and maintained the steady ΔT value for reasonable permeate flux value. DCMD was operation at relatively low temperatures from 70-90 ºC and 99% salt rejection was achieved in modified DCMD system. In our study PTFE showed maximum flux at high feed temperature whereas PVDF attainedcompete separation of salts at relatively lower ΔT value with a short period of time. So, this could be more economical for scale-up processes. Future researches were going on to modify the membrane properties by using of nanoparticles for better MD process.

➢ Future scope of work

MD has been investigated since the early 1960s, but in the last decade it has shown remarkable development in different treatment processes. One of the major focus of this process is to minimize thermal energy demand.MD has been used mainly for removing salt from sea water and brackish water. It can also be applied for removal of other contaminants, such as heavy metals, radionuclides, and organics from brackish, produced, industrial and other impurities from water. However, reverse osmosis finds difficulty to treat highly concentrated brine solution, in such case MD may be integrated with RO for better removal.

Finding suitable applications for MD in commercial purpose is one of the scopes for its future work. As it can be operated at low temperature, renewable energy like solar energy, waste energy etc. can be introduced to reduce the cost efficiency.

Low fluxes, pore wetting, high liquid entry pressure have been found as limitations for MD process. Membrane hydrophobicity, surface energy, pore geometry are critical parameters for mass transfer and pore wetting. Pore wetting and fouling can be reduced by oleophobic coatings. Membrane modification can be done by using nanocomposition of TiO_2 and polystyrene. Also membranes can be improved by using low temperature hydrothermal process followed by surface flourosilanization, where Zinc oxide can be used as base compound.

Electronics technology can be introduced for mathematical modelling of DCMD process.

References

Alkhudhiri, A., Darwish, N., & Hilal, N. (2012). Membrane distillation: a comprehensive review. *Desalination*, *287*, 2-18.

Anderson, A. J., & Dawes, E. A. (1990). Occurrence, metabolism, metabolic role, and industrial uses of bacterial polyhydroxyalkanoates. *Microbiology and Molecular Biology Reviews*, *54*(4), 450-472.

Ashoor, B. B., Mansour, S., Giwa, A., Dufour, V., & Hasan, S. W. (2016). Principles and applications of direct contact membrane distillation (DCMD): a comprehensive review. *Desalination*, *398*, 222-246.

Bhattacharyya, A., Jana, K., Haldar, S., Bhowmic, A., Mukhopadhyay, U. K., De, S., & Mukherjee, J. (2015). Integration of poly-3-(hydroxybutyrate-co-hydroxyvalerate) production by Haloferax mediterranei through utilization of stillage from rice-based ethanol manufacture in India and its techno-economic analysis. *World Journal of Microbiology and Biotechnology*, *31*(5), 717-727.

Bhattacharyya, A., Pramanik, A., Maji, S. K., Haldar, S., Mukhopadhyay, U. K., & Mukherjee, J. (2012). Utilization of vinasse for production of poly-3-(hydroxybutyrate-co-hydroxyvalerate) by Haloferax mediterranei. *AMB express*, *2*(1), 34.

Bhattacharyya, A., Saha, J., Haldar, S., Bhowmic, A., Mukhopadhyay, U. K., & Mukherjee, J. (2014). Production of poly-3-(hydroxybutyrate-co-hydroxyvalerate) by Haloferax mediterranei using rice-based ethanol stillage with simultaneous recovery and re-use of medium salts. *Extremophiles*, *18*(2), 463-470.

Boubakri, A., Hafiane, A., & Bouguecha, S. A. T. (2014). Application of response surface methodology for modeling and optimization of membrane distillation desalination process. *Journal of Industrial and Engineering Chemistry*, *20*(5), 3163-3169.

Bugnicourt, E., Cinelli, P., Lazzeri, A., & Alvarez, V. A. (2014). Polyhydroxyalkanoate (PHA): Review of synthesis, characteristics, processing and potential applications in packaging.

Camacho, L., Dumée, L., Zhang, J., Li, J. D., Duke, M., Gomez, J., & Gray, S. (2013). Advances in membrane distillation for water desalination and purification applications. *Water*, *5*(1), 94-196.

Chen, G., Zhang, G., Park, S., & Lee, S. (2001). Industrial scale production of poly (3-hydroxybutyrate-co-3-hydroxyhexanoate). *Applied microbiology and biotechnology*, *57*(1-2), 50-55.

Davey, B., & Priestley, H. (1990). Introduction to Lattices and Order Cambridge Univ. *Press, Cambridge*.

Dow, N., Zhang, J., Duke, M., Li, J. D., Gray, S. R., & Ostarcevic, E. (2008). Membrane distillation of brine wastes.

Drioli, E., Ali, A., & Macedonio, F. (2015). Membrane distillation: Recent developments and perspectives. *Desalination*, *356*, 56-84.

Elimelech, M., & Phillip, W. A. (2011). The future of seawater desalination: energy, technology, and the environment. *science*, *333*(6043), 712-717.

Giwa, A., Akther, N., Dufour, V., & Hasan, S. W. (2016). A critical review on recent polymeric and nano-enhanced membranes for reverse osmosis. *Rsc Advances*, *6*(10), 8134-8163.

Gomez, J. G. C., Rodrigues, M. F. A., Alli, R. C. P., Torres, B. B., Netto, C. B., Oliveira, M. S., & Da Silva, L. F. (1996). Evaluation of soil gram-negative bacteria yielding polyhydroxyalkanoic acids from carbohydrates and propionic acid. *Applied microbiology and biotechnology*, *45*(6), 785-791.

Gonda, T. J., Buckmaster, C., & Ramsay, R. G. (1989). Activation of c-myb by carboxy-terminal truncation: relationship to transformation of murine haemopoietic cells in vitro. *The EMBO journal*, *8*(6), 1777-1783.

Gryta, M. (2005). Long-term performance of membrane distillation process. *Journal of Membrane Science*, *265*(1-2), 153-159.

Hahn, S. K., Chang, Y. K., & Lee, S. Y. (1995). Recovery and characterization of poly (3-hydroxybutyric acid) synthesized in Alcaligenes eutrophus and recombinant Escherichia coli. *Appl. Environ. Microbiol.*, *61*(1), 34-39.

Kampa, M., & Castanas, E. (2008). Human health effects of air pollution. *Environmental pollution*, *151*(2), 362-367.

Kim, A. S. (2013). A two-interface transport model with pore-size distribution for predicting the performance of direct contact membrane distillation (DCMD). *Journal of membrane science*, *428*, 410-424.

Koo, J., Han, J., Sohn, J., Lee, S., & Hwang, T. M. (2013). Experimental comparison of direct contact membrane distillation (DCMD) with vacuum membrane distillation (VMD). *Desalination and Water Treatment*, *51*(31-33), 6299-6309.

Kusaka, S., Abe, H., Lee, S., & Doi, Y. (1997). Molecular mass of poly [(R)-3-hydroxybutyric acid] produced in a recombinant Escherichia coli. *Applied Microbiology and Biotechnology*, *47*(2), 140-143.

Lasemi, Z., Darzi, G. N., & Baei, M. S. (2013). Media optimization for poly (β-hydroxybutyrate) production using Azotobacter Beijerinckii. *International Journal of Polymeric Materials and Polymeric Biomaterials*, *62*(5), 265-269.

Lee, K. P., Arnot, T. C., & Mattia, D. (2011). A review of reverse osmosis membrane materials for desalination—development to date and future potential. *Journal of Membrane Science*, *370*(1-2), 1-22.

Lee, S. Y. (1996). Bacterial polyhydroxyalkanoates. *Biotechnology and bioengineering*, *49*(1), 1-14.

Manawi, Y. M., Khraisheh, M., Fard, A. K., Benyahia, F., & Adham, S. (2014). Effect of operational parameters on distillate flux in direct contact membrane distillation (DCMD): Comparison between experimental and model predicted performance. *Desalination*, *336*, 110-120.

Markert, B., Wuenschmann, S., Fraenzle, S., Figueiredo, A. M. G., Ribeiro, A. P., & Wang, M. (2011). Bioindication of atmospheric trace metals–With special references to megacities. *Environmental pollution*, *159*(8-9), 1991-1995.

Martínez, L., Florido-Díaz, F. J., Hernandez, A., & Prádanos, P. (2002). Characterisation of three hydrophobic porous membranes used in membrane distillation: Modelling and evaluation of their water vapour permeabilities. *Journal of membrane science*, *203*(1-2), 15-27.

Nakoa, K., Date, A., & Akbarzadeh, A. (2016). DCMD modelling and experimental study using PTFE membrane. *Desalination and Water Treatment*, *57*(9), 3835-3845.

Pangarkar, B. L., Sane, M. G., & Guddad, M. (2011). Reverse osmosis and membrane distillation for desalination of groundwater: a review. *ISRN Materials Science*, *2011*.

Poli, A., Di Donato, P., Abbamondi, G. R., & Nicolaus, B. (2011). Synthesis, production, and biotechnological applications of exopolysaccharides and polyhydroxyalkanoates by archaea. *Archaea*, *2011*.

Pötter, M., & Steinbüchel, A. (2005). Poly (3-hydroxybutyrate) granule-associated proteins: impacts on poly (3-hydroxybutyrate) synthesis and degradation. *Biomacromolecules*, *6*(2), 552-560.

Qtaishat, M., Matsuura, T., Kruczek, B., & Khayet, M. (2008). Heat and mass transfer analysis in direct contact membrane distillation. *Desalination*, *219*(1-3), 272-292.

Qu, D., Sun, D., Wang, H., & Yun, Y. (2013). Experimental study of ammonia removal from water by modified direct contact membrane distillation. *Desalination*, *326*, 135-140.

Quillaguamán, J., Guzmán, H., Van-Thuoc, D., & Hatti-Kaul, R. (2010). Synthesis and production of polyhydroxyalkanoates by halophiles: current potential and future prospects. *Applied Microbiology and Biotechnology*, *85*(6), 1687-1696.

Quillaguaman, J., Hashim, S., Bento, F., Mattiasson, B., & Hatti-Kaul, R. (2005). Poly (β-hydroxybutyrate) production by a moderate halophile, Halomonas boliviensis LC1 using starch hydrolysate as substrate. *Journal of applied microbiology*, *99*(1), 151-157.

Ramsay, J. A., Berger, E., Ramsay, B. A., & Chavarie, C. (1990). Recovery of poly-3-hydroxyalkanoic acid granules by a surfactant-hypochlorite treatment. *Biotechnology Techniques*, *4*(4), 221-226.

Rao, G., Hiibel, S. R., & Childress, A. E. (2014). Simplified flux prediction in direct-contact membrane distillation using a membrane structural parameter. *Desalination*, *351*, 151-162.

Ray, A., Cot, M., Puzo, G., Gilleron, M., & Nigou, J. (2013). Bacterial cell wall macroamphiphiles: pathogen-/microbe-associated molecular patterns detected by mammalian innate immune system. *Biochimie*, *95*(1), 33-42.

Sabino, A., Hewitt, J., & Petrow, W. (2009). *U.S. Patent No. 7,511,611*. Washington, DC: U.S. Patent and Trademark Office.

Schaefer, A., Fane, A. G., & Waite, T. D. (Eds.). (2005). *Nanofiltration: principles and applications*. Elsevier.

Scott, K. (1995). *Handbook of industrial membranes*. Elsevier.

Shahid, S., Mosrati, R., Ledauphin, J., Amiel, C., Fontaine, P., Gaillard, J. L., & Corroler, D. (2013). Impact of carbon source and variable nitrogen conditions on bacterial biosynthesis of polyhydroxyalkanoates: evidence of an atypical metabolism in Bacillus megaterium DSM 509. *Journal of bioscience and bioengineering*, *116*(3), 302-308.

Smolders, K. F. A. C. M., & Franken, A. C. M. (1989). Terminology for membrane distillation. *Desalination*, *72*(3), 249-262.

Smolders, K. F. A. C. M., & Franken, A. C. M. (1989). Terminology for membrane distillation. *Desalination*, *72*(3), 249-262.

Susanto, H. (2011). Towards practical implementations of membrane distillation. *Chemical Engineering and Processing: Process Intensification*, *50*(2), 139-150.

Tijing, L. D., Woo, Y. C., Choi, J. S., Lee, S., Kim, S. H., & Shon, H. K. (2015). Fouling and its control in membrane distillation—A review. *Journal of Membrane Science*, *475*, 215-244.

Tomaszewska, M., & Łapin, A. (2012). The influence of feed temperature and composition on the conversion of KCl into KHSO4 in a membrane reactor combined with direct contact membrane distillation. *Separation and purification technology*, *100*, 59-65.

Wang, F., & Lee, S. Y. (1997). Poly (3-Hydroxybutyrate) Production with High Productivity and High Polymer Content by a Fed-Batch Culture of Alcaligenes latus under Nitrogen Limitation. *Appl. Environ. Microbiol.*, *63*(9), 3703-3706.

Warsinger, D. M., Swaminathan, J., Guillen-Burrieza, E., & Arafat, H. A. (2015). Scaling and fouling in membrane distillation for desalination applications: a review. *Desalination*, *356*, 294-313.

Yu, H., Yang, X., Wang, R., & Fane, A. G. (2012). Analysis of heat and mass transfer by CFD for performance enhancement in direct contact membrane distillation. *Journal of membrane science*, *405*, 38-47.

Zhang, J., & Gray, S. (2011). Effect of applied pressure on performance of PTFE membrane in DCMD. *Journal of Membrane Science*, *369*(1-2), 514-525.

Zhang, J., & Gray, S. (2012). Modelling heat and mass transfers in DCMD using compressible membranes. *Journal of membrane science*, *387*, 7-16.